

FINAL REPORT

on

POINT BEACH NUCLEAR PLANT UNIT NO. 2
PRESSURE VESSEL SURVEILLANCE PROGRAM:
EVALUATION OF CAPSULE V

to

WISCONSIN ELECTRIC POWER COMPANY

June 10, 1975

by

J. S. Perrin, D. R. Farmelo, L. M. Lowry
R. O. Wooton, and R. S. Denning

BATTELLE
Columbus Laboratories
505 King Avenue
Columbus, Ohio 43201

8803020125 880226
PDR FOIA
CONNOR88-45 PDR

B/2

TABLE OF CONTENTS

	<u>Page</u>
SUMMARY.	1
INTRODUCTION	2
CAPSULE RECOVERY AND DISASSEMBLY	5
SAMPLE PREPARATION	8
Pressure Vessel Material.	8
Correlation Monitor Material.	8
EXPERIMENTAL PROCEDURES.	9
Dosimeter and Thermal Monitor Examination	9
Tensile Properties.	11
Charpy Impact Properties.	14
RESULTS AND DISCUSSION	17
Dosimeter and Thermal Monitor Examination	17
Tensile Properties.	27
Charpy Impact Properties.	37
CONCLUSIONS.	56
REFERENCES	57

APPENDIX A

PRESSURE VESSEL MATERIAL	A-1
------------------------------------	-----

APPENDIX B

ASTM CORRELATION MONITOR MATERIAL.	B-1
--	-----

APPENDIX C

DOSIMETER COUNTING DATA.	C-1
----------------------------------	-----

APPENDIX D

DOSIMETER AND CAPSULE EXAMINATION.	D-1
--	-----

APPENDIX E

INSTRUMENTED CHARPY PROPERTIES.	E-1
---	-----

APPENDIX F

WOL FRACTURE TOUGHNESS PROPERTIES.	F-1
--	-----

POINT BEACH NUCLEAR PLANT UNIT NO. 2
PRESSURE VESSEL SURVEILLANCE PROGRAM:
EVALUATION OF CAPSULE V

by

J. S. Perrin, D. R. Farmelo, L. M. Lowry,
R. O. Wooton, and R. S. Denning

SUMMARY

The irradiation conditions and the irradiation induced changes in mechanical properties of the Point Beach Unit No. 2 reactor pressure vessel have been determined from evaluation of specimens contained in Capsule V. This capsule contained base metal, weld metal, and heat-affected-zone metal specimens. The capsule was removed after 1.52 equivalent full-power years of operation. The irradiation temperature did not exceed 590 F, and the capsule received a fluence of 4.74×10^{18} nvt (>1 MeV).

The measured changes in the 30 ft-lb and 50 ft-lb Charpy impact transition temperature for the three reactor materials were consistent with those observed for other programs involving similar materials and irradiation conditions. Of particular interest is the upper shelf energy level drop from a preirradiation value of approximately 65 ft-lb to an irradiated value of 42 ft-lb. A trend band for the change in the 30 ft-lb and 50 ft-lb transition temperature with increasing exposure to fast neutrons was determined from the results of this program and those of other programs. The tensile specimen examination showed that, in general, the yield and ultimate tensile strengths of the materials examined increased and that the reduction in area and the total elongation decreased.

INTRODUCTION

This report presents the results of the examination of Capsule V, the first capsule of the continuing surveillance program for monitoring the effects of neutron irradiation on the A508 Grade B Point Beach Unit No. 2 reactor pressure-vessel material under actual operating conditions. This report contains experimental procedures, results, and discussion relating to the investigation.

Radiation damage studies initiated during the early days of nuclear power-reactor development revealed the deleterious effects of high energy neutrons upon the notch ductility of reactor vessel steels. The effect was characterized by a rapid rise in the transition temperature with increasing neutron exposure. In addition, the tensile properties show a significant increase in yield strength and tensile strength, accompanied by a loss of uniform elongation and reduction of area with increasing neutron exposure.

Sufficient data on the effects of radiation on the mechanical properties of reactor pressure-vessel steel are now available to indicate the type and relative magnitude of property changes to be encountered during the expected lifetime of the reactor structure. This information is an integral part of the design basis for a nuclear reactor. During the reactor life the operating limitation curves (i.e., pressure and temperature) will be periodically adjusted to incorporate the projected changes in mechanical properties.

To further ensure the continued safe operations of the plant, a reactor-vessel radiation-surveillance program is being conducted. The primary purpose of this program is to evaluate the specific changes in the mechanical properties of the pressure-vessel materials under the actual service conditions (neutron fluence, time, and temperature) of the reactor plant. It is known that the magnitude and relationships of the property changes are functions of the specific material composition and metallurgical condition; the amount, rate, and energy spectrum of the radiation; and

the exposure temperature^{(1-7)*}. The surveillance program is designed to provide information for determining whether the reactor pressure-vessel operating limitations are indeed conservative, as is expected.

The surveillance program for the reactor was designed and recommended by the Westinghouse Electric Corporation and is based on ASTM E 185, "Surveillance Tests on Structural Materials in Nuclear Reactors"⁽⁸⁾. The details of this program and the preirradiation mechanical properties of the materials are presented in Reference (9). Prior to start-up, six capsules containing tensile, Charpy V-notch, and WOL fracture-mechanics specimens of the pressure-vessel materials were installed in the reactor. The capsules were located between the thermal shield and the vessel wall. In addition to these mechanical-property test specimens, the capsules contain thermal-monitor and neutron-fluence specimens for evaluation of the specific temperature and radiation exposure conditions of the specimens.

The particular exposure condition variables evaluated are the total integrated fast fluence of the capsule and the maximum temperature encountered by the specimens during the exposure period. The temperature history of the surveillance capsule is fairly representative of that encountered by the pressure-vessel wall. However, the capsule is a finite distance from the reactor pressure-vessel wall, and therefore the capsule receives an accelerated fluence as compared to the vessel wall.

The most essential mechanical properties evaluated by the test specimens in the surveillance capsule are the ductile-to-brittle fracture transition temperature and the conventional tensile-strength and ductility values. In this context, essential refers to those requirements of the current methods for establishing pressure-temperature operating limitations of the reactor pressure vessel. An essential requirement of the mechanical property measurements is that they be made on representative material.

*References at end of text.

For this surveillance program, the capsules contain test specimens of the A508 Class 2 reactor-vessel steel from two 6-1/2 in. thick shell plates from the vessel intermediate and lower shell courses, and also representative weld metal and heat-affected-zone (HAZ) metal. The thermal history of the material used to fabricate test specimens is as identical as possible to that received by the reactor pressure vessel during fabrication.

The surveillance capsule being examined contained not only Charpy specimens machined from pressure vessel metal used in the reactor under examination, but also ASTM correlation monitor Charpy specimens. These specimens are in numerous commercial power reactor surveillance capsules. By comparing the results of the correlation monitor specimens from numerous surveillance programs, further knowledge should be gained concerning the effect of differing nuclear irradiation conditions (neutron spectrum and flux intensity) on the radiation response of reference correlation monitor steels.⁽⁵⁾

The main text of the report contains the results of the thermal monitor and neutron dosimeter examination, the Charpy impact specimen examination, and the tensile specimen examination. The WOL specimen examination is presented in an appendix to the report.

CAPSULE RECOVERY AND DISASSEMBLY

Battelle's Columbus Laboratories (BCL) personnel went to the Point Beach Nuclear Plant Unit No. 2 to pick up the surveillance capsule assembly. They brought a pool-side jib crane, a specialized underwater cutting tool, and a shipping cask. The cutting head of the underwater cutting tool is a mild steel casting. The head had been sand blasted, copper plated, and then nickel plated to prevent it from rusting and thereby contaminating the pool water. To further avoid contamination, pool water was used in the line leading from the pump intensifier unit to the cutting head.

The capsule assembly had an overall length of approximately 130 inches. Point Beach personnel removed the capsule assembly from the pressure vessel and transferred it underwater in a canal to the spent fuel pool. The upper lid and lower drain lid were removed from the shipping cask. Using an overhead crane, the cask was then raised from the receiving area, moved to a position over the spent fuel pool, and lowered into the pool so that the bottom end of the cask was resting on the floor of the pool. The Point Beach handling tool attached to the bridge crane was then used to position the square capsule, with the attached round lead tube, at the bottom of the shipping cask. Westinghouse drawing number 686J468 showed the internal cask cavity to be approximately 95 inches deep and the upper lid depth to be 8 inches.

The cutting tool was lowered into the pool using a stainless steel cable attached to the pool-side jib crane. The cutter was guided into position using the stainless steel pipe line leading to the cutting head. The capsule was raised about 35 inches and binoculars were used to determine the position of the cutting head. The first sectioning cut was then made. After cutting, it was determined that the capsule had been cut on the square capsule section. A second cut was made separating the lead tube into two sections. These two sections were placed into the cask along side the lower capsule section.

The cask was raised from the pool and its exterior was thoroughly rinsed with water. The water inside the cask was allowed to drain into the pool. The overhead crane was then used to lower the cask to the decontamination area. The cask was decontaminated to the level of removable contamination required for shipping, 2200 disintegrations/100 cm²/min $\beta\gamma$ and 220 disintegrations/100 cm²/min α . The cask was then shipped to the BCL Hot Laboratory Facility by commercial carrier.

Upon arrival at BCL, the cask was placed in a hot cell. The three capsule and lead tube sections were then removed from the cask. The capsule sections were examined and measurements indicated the first cut had been made at about 54 in. from the capsule bottom in the region of a WOL specimen. Visual examination showed the capsule to be a dark gray color with the identification mark "V" stamped on the lower end of the capsule.

The specimens were removed from the capsule and inventoried. The appearance of the specimens was a dark gray color and it was found that one WOL had been severed during the reactor site cutting operation. The specimen inventory is shown in Table 1, which is in agreement with WCAP 7712⁽⁹⁾. Before testing, the mechanical property specimens were cleaned in the following manner:

1. Prewashed in a solution of Radiac and water
2. Ultrasonically cleaned for a minimum of 45 minutes in a solution of detergent and water
3. Removed from ultrasonic bath, rinsed with clean water, and then rinsed with reagent grade alcohol.

EXPERIMENTAL PROCEDURES

This section describes the procedures employed in the testing of the impact and tensile specimens. Also included are the procedures used to examine the dosimeters and thermal monitors. All experimental examinations and evaluations were conducted at Battelle's Columbus Laboratories.

Dosimeter and Thermal Monitor Examination

The capsule contained two kinds of low-melting-point eutectic alloy thermal monitor wires for determination of the maximum temperature attained by the test specimens during irradiation. One alloy was 2.5% Ag-97.5% Pb with a melting point of 579 F. The other alloy was 1.75% Ag-0.75% Sn-97.5% Pb with a melting point of 590 F. These thermal monitor alloys were sealed in Pyrex tubes and inserted in spacers in the capsule. During capsule disassembly the thermal monitor wires were removed from the spacers and Pyrex tubes. The wires were then visually examined for evidence of melting at a magnification of 4X using a stereomicroscope.

The capsule contained a total of 22 dosimeters of copper, nickel, cadmium-shielded aluminum-cobalt alloy, unshielded aluminum-cobalt alloy, neptunium 237 and uranium 238 in three locations. Included are the iron dosimeters, obtained from actual Charpy or tensile test specimens. The reactions used for the dosimetry calculations were as follows:

Iron	^{54}Fe (n,p)	^{54}Mn
Nickel	^{58}Ni (n,p)	^{58}Co
Copper	^{63}Cu (n, α)	^{60}Co
Cobalt	^{59}Co (n, γ)	^{60}Co
Uranium	^{238}U (n,f)	^{137}Cs
Neptunium	^{237}Np (n,f)	^{137}Cs

All 22 dosimeter samples were analyzed. The composition of the impurities of the medium surrounding the dosimeter monitor specimens was not stated in Reference (9) and is not known.

After removal from the capsule, the individual samples were placed in vials for transfer to the radiochemistry laboratory. Radiation readings at 1 meter and on contact were recorded. The nickel, copper, and cobalt wires were decontaminated by wiping with dilute acid, distilled water, and reagent grade acetone. The iron samples and ^{238}U and ^{237}Np capsules were wiped with dilute acid and distilled water to remove major contamination and then cleaned ultrasonically in a solution of Radiac and water.

The copper, nickel, and Al-0.15 Co wires were weighed to ± 0.0001 g, and the activation product intensities were determined directly by gamma ray spectrometry. For the iron samples drillings were taken through a complete cross section near the center of the designated Charpy impact or tensile specimen. The drillings were then weighed and mounted on a standard counting ring and gamma counted.

^{238}U and ^{237}Np capsules were opened in an alpha radiation containment box by specially prepared tools used to grip the small 1/4 in. diameter x 3/8 in. long cylinders and cut off the tops. The tool used for cutting off the tops was a modified tubing cutter. The ^{238}U and ^{237}Np were present in the form of oxide powders. The two samples were poured into small tared primary containment vials and then into clean tared secondary vials for weighing to ± 0.0001 g on an analytical balance. They were dissolved in 8M HNO_3 (U_3O_8) and 8M H_2SO_4 - 0.1M NaBrO_3 (NpO_2), and diluted to appropriate volumes. ^{137}Cs analyses were performed in duplicate by pipeting 1 ml aliquots into plastic vials and counting with a high resolution, lithium drifted germanium detector. NBS ^{137}Cs standards in identical form were utilized to obtain the appropriate disintegration rates. Utilizing this method a ^{137}Cs separation is not necessary since it is resolved from ^{134}Cs and other fission product activities.

The remaining activation products were analyzed by gamma-ray spectrometry utilizing a 3 in. diameter x 3 in. long NaI (Tl) scintillation crystal detector and model 401D 400 channel analyzer (Technical Measurements Corp) capable of 7 percent resolution FWHM (full width half maximum) at the 0.663 MeV ^{137}Cs - $^{137\text{m}}\text{Ba}$ gamma ray energy level. The ^{54}Mn , ^{60}Co , and ^{137}Cs samples were counted directly against NBS standards. The ^{58}Co activity was obtained from comparison with theoretical efficiency curves prepared from NBS standards.

The procedures used in the evaluation of the dosimetry samples followed the appropriate ASTM recommendations⁽¹⁰⁻¹⁶⁾.

Tensile Properties

The design of the tensile specimens is shown in Figure 1. The gage section has a nominal 0.250 in. diameter and a nominal 1.000 in. length. Tensile properties were determined using a Model TT-D Instron machine. The machine has a 20,000 lb capacity. During tests a crosshead speed of 0.05 in. per min was used. An elastic strain gage tensile bar built at Battelle-Columbus and calibrated against NBS proving rings was used to calibrate the loading system of the Instron over a 0 to 10,000 lb range. The gripping devices used to grip the ends of the tensile specimen are pin-type units made at Battelle-Columbus.

The deformation of the specimen was measured using a Baldwin Series 200 high temperature extensometer. An Instron Model G51-12A strain gage unit is part of the extensometer. The strain gage unit senses the differential movement of two extensometer extension arms attached to the specimen gage length 1 in. apart. The extension arms are required for thermal protection of the strain gage unit during the elevated temperature tests. Figure 2 shows the extensometer extension arms and strain gage assembly used for tensile testing. A tensile specimen is shown at the top of the figure next to the region of the extension arms where the specimen is loaded for testing. The strain gage unit is shown at the bottom of the figure next to the region of the extensometer arms where the unit is attached during testing. The extensometer was calibrated before testing using an Instron Extensometer Calibrator. The load and elongation were recorded on the recorder unit which is an integral part of the Instron machine. Curves were run in a load-elongation mode until the vicinity of maximum load. The curves were then finished in a load-time mode so that a complete curve would be generated in case of extensometer slippage after the specimen started to neck down locally.

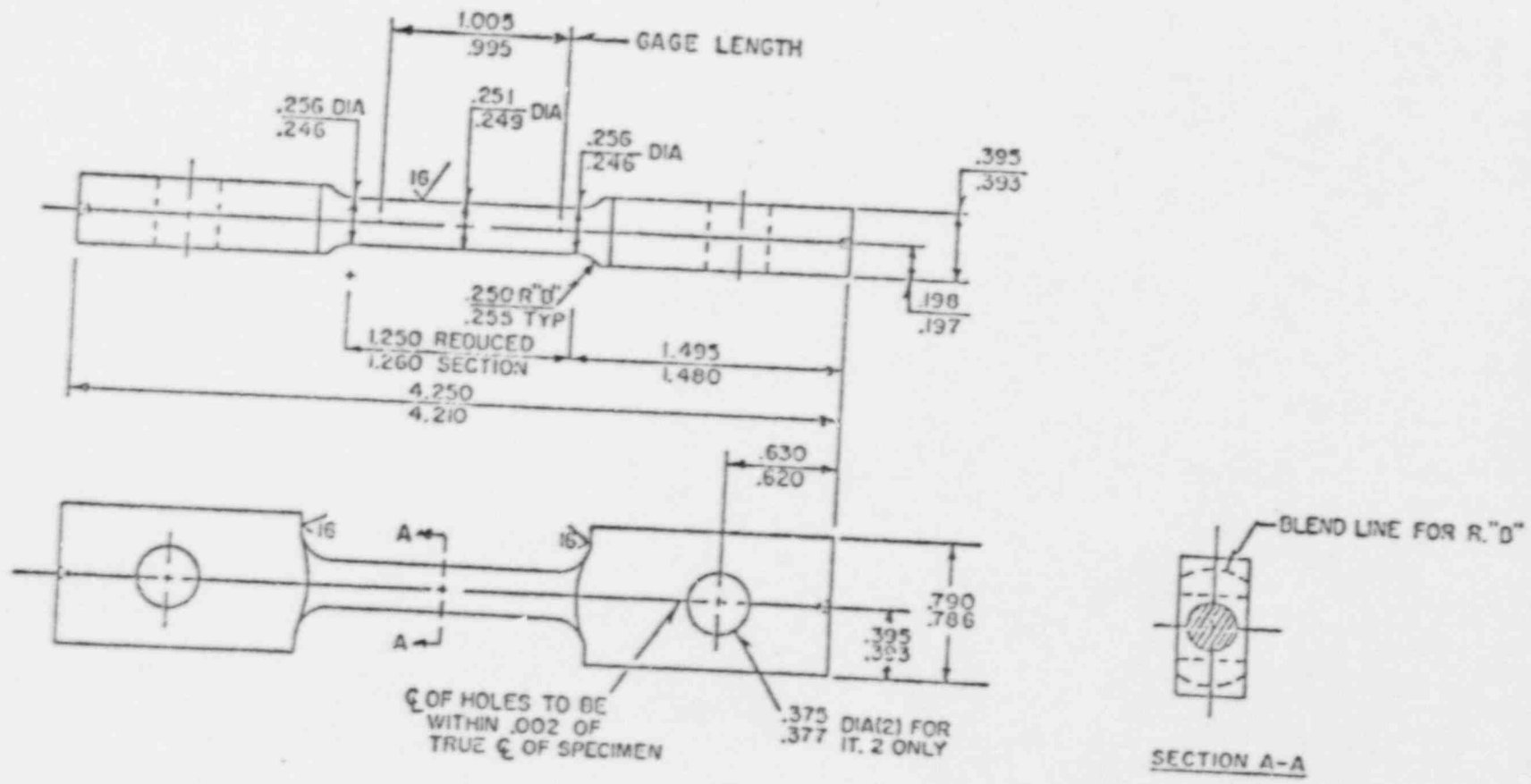
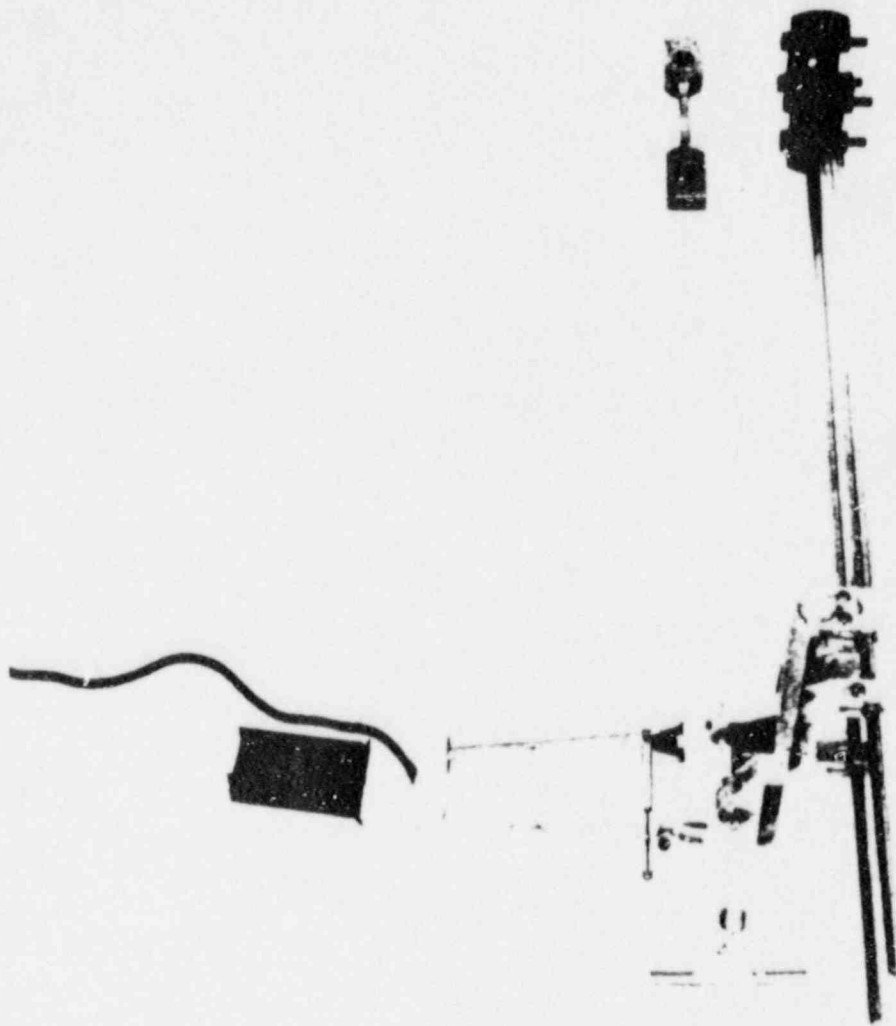


FIGURE 1. TENSILE SPECIMEN



P4973

FIGURE 2. EXTENSOMETER EXTENSION ARMS AND STRAIN GAGE
ASSEMBLY USED FOR TENSILE TESTING

Elevated temperature tensile tests were conducted using a three-zone split furnace. The irradiated tensile specimens were tested at room temperature, 300 F, and 550 F. The specimens were held at temperature before testing to stabilize the temperature. Temperature was monitored using a Chromel-Alumel thermocouple in direct contact with the gage section of the specimen.

The load-extension data were recorded on the testing machine strip chart. The yield strength, ultimate tensile strength, and total elongation were determined from these charts. The reduction in area was determined from specimen measurements made using a vernier caliper. The yield strength was determined by drawing a line parallel to the elastic region of the stress-strain curve. The line was drawn offset to the curve at a distance of 0.2% strain.

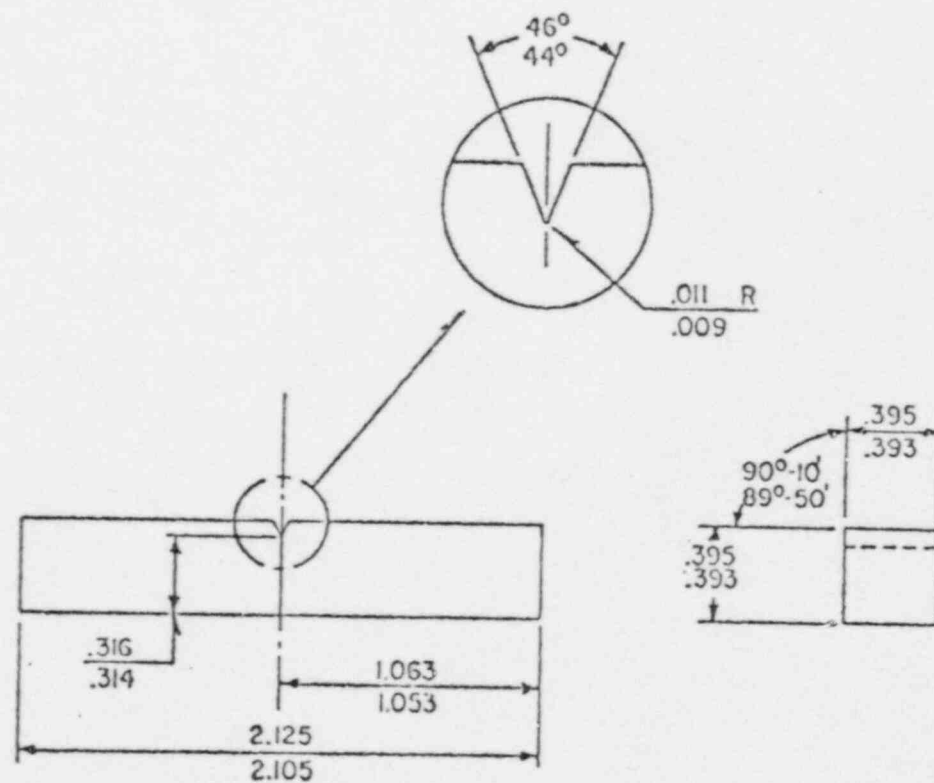
Charpy Impact Properties

The Charpy impact tests were conducted using a 240 ft-lb Satec-Baldwin Model SI-1C impact machine in accordance with ASTM E23-72⁽¹⁷⁾. Standard specimens of the design shown in Figure 3 were used. The 240 ft-lb range was used for all tests. The velocity of the hammer at impact was 17.0 ft/sec. The impact machine was checked and calibrated by a representative of the manufacturer. The calibration of the machine was then verified as specified in ASTM E23-72 using Charpy impact specimens purchased from the U.S. Army Materials Research Agency. The results, listed in Table 2, confirmed the machine was calibrated.

TABLE 2. CALIBRATION DATA FOR THE BCL HOT
LABORATORY CHARPY IMPACT MACHINE

Group	Average BCL Energy, ft-lb	Standard Energy, (a) ft-lb	Variation	
			Actual	Allowed
Low Energy	13.3	13.3	0 ft-lb	±1.0 ft-lb
Medium Energy	49.0	50.7	-3.4%	±5.0%
High Energy	74.7	77.3	-3.4%	±5.0%

(a) Established by U.S. Army Materials and Mechanics Research Center.



$\sqrt[63]{}$ ALL OVER UNLESS OTHERWISE SPECIFIED

FIGURE 3. CHARPY V-NOTCH IMPACT SPECIMEN

The impact machine was inspected each day during use to determine the energy loss due to friction. This was done by the following: (a) releasing the pendulum from the 240 ft-lb upright position with no specimen in the machine and determining the indicated energy value is 0 ft-lb; (b) without resetting the pointer, again releasing the pendulum from the 240 ft-lb upright position and permitting it to swing 11 half cycles. After the pendulum starts its 11th cycle, the pointer is moved to between 12 and 24 ft-lbs and it is determined that the indicated value, divided by 11, does not exceed 0.4 percent (9.6 ft-lb) of the 240 ft-lb capacity.

ASTM procedures for specimen temperature control were utilized. The low temperature bath consisted of agitated methyl alcohol cooled with additions of liquid nitrogen. The container was a Dewar flask which contained a grid to keep the specimens at least 1 in. from the bottom. The height of the bath was enough to keep a minimum of 1 in. of liquid over the specimens. The Charpy specimens were held at temperature for a minimum of at least the ASTM recommended time.

The tests above room temperature were conducted in a similar manner except that a metal container with a liquid bath was used. The bath used for temperatures from 70 to 212 F was water, and the bath used for temperatures above 212 F was oil. The baths were heated to temperature using a hot plate.

The specimens were manually transferred from the temperature bath to the anvil of the impact machine by means of tongs that had also been brought to temperature in the bath. The specimens were removed from the bath and impacted in less than 5 sec. The energy required to break the specimens was recorded and plotted as a function of test temperature as the testing proceeded.

Lateral expansion was determined from measurements made with a lateral expansion gage. Fracture appearance was estimated from observation of the fracture surface, and comparing the appearance of the specimen to an ASTM fracture appearance chart⁽¹⁸⁾.

RESULTS AND DISCUSSION

Dosimeter and Thermal Monitor Examination

The capsule contained three 579 F and two 590 F thermal monitors. The 579 F monitors were located in the top, middle, and bottom regions of the capsule. One 590 F monitor, referred to as the top-middle monitor, was located between the top and middle regions of the capsule. The other 590 F monitor, referred to as the bottom-middle monitor, was located between the bottom and middle regions of the capsule.

Monitors were examined at a magnification of 4X using a stereo-microscope. The middle 579 F monitor showed no evidence of melting. This monitor had a cross section which was approximately rectangular. The four faces were flat, and the edges were sharp and well defined. The top 579 F monitor had three faces along the length. Two were flat, but the third was melted as though some melting may have occurred. Figure 4A shows the two relatively flat surfaces. The bottom 579 F monitor showed obvious melting along the complete length. There were areas along the length which were rounded, and were smooth and shiny. Figure 4B shows the monitor. It was both shorter and larger in diameter as compared to the other two 579 F monitors. The cross section along most of the length of the top-middle 590 F monitor appears to be rectangular with flat surfaces and sharp edges. However, at one end there appears to have been a slight amount of melting, which may have occurred when the Pyrex tube was sealed. This monitor was definitely not at or above 590 F along the length because there is no evidence of general melting. The bottom-middle 590 F monitor appears to have at least partially melted, since there is rounding along one edge of the complete length. In addition, one end shows some evidence of melting. This monitor is shown in Figure 4C. The slight curve along the complete length is a result of the monitor being bent slightly on removal from the Pyrex capsule.



FIGURE 4a. TOP 579 F THERMAL MONITOR

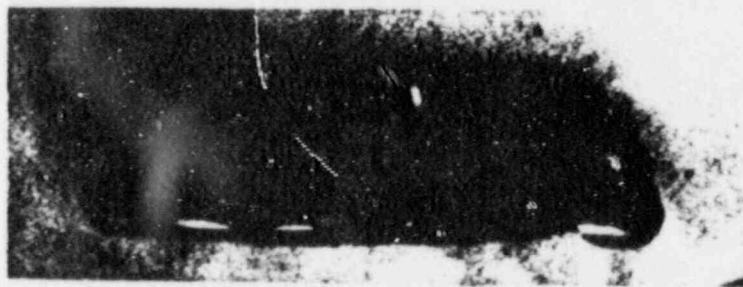


FIGURE 4b. BOTTOM 579 F MONITOR



FIGURE 4c. BOTTOM-MIDDLE 590 F MONITOR

The results of the thermal monitor examination indicate some melting of 579 F monitors occurred including general melting of one 579 F monitor. However, there was no general melting of the 590 F monitors. Therefore the surveillance capsule appears to have been below 590 F during irradiation.

The surveillance capsule was in the reactor for 556 equivalent full power days or 1.52 equivalent full power years, based on a full power output of 1518 Mw(t).⁽¹⁹⁾ The positions in the reactor of capsule V and the other surveillance program capsules shown in Figure 5. Capsule V had an exposure lead factor with respect to the inner surface at the pressure vessel wall of 2.5.⁽²⁰⁾

All 12 fast neutron monitors and 10 thermal neutron monitors were counted for gamma ray activity to determine integrated fast fluence and thermal fluence, respectively. The fast flux monitors are iron, nickel, copper, uranium and neptunium, and the results are shown in Table 3. Fast fluence values ($E > 1$ MeV) for Ni, Fe, and Cu were 3.80×10^{18} , 4.74×10^{18} and 4.76×10^{18} n/cm², respectively. Neptunium and uranium values were 7.79×10^{18} and 8.24×10^{18} n/cm², respectively. Because the iron samples are from actual Charpy or tensile test specimens and the nuclear constants are well established, the average iron fast fluence ($E > 1$ MeV) of 4.74×10^{18} n/cm² is considered most representative of the five monitors. The copper monitor confirms this value. Nickel dosimetry results are not reliable for long term irradiations due to its relatively short half-life of 71.3 days (Co^{58}). The Np-237 and U-238 monitors resulted in values 60-70 percent higher than the Fe results. These values tend to run higher than average and it is believed due to uncertainty in cross sections and threshold values in the relatively new procedures. The Np-237 procedure is presently undergoing evaluation by ASTM.

The Point Beach Unit No. 2 Technical Specification indicates that 0.891×10^6 Mw(t)-days of operation is equivalent to 1.9×10^{18} n/cm (> 1 MeV).⁽²¹⁾ Based on the capsule exposure lead factor of 2.5, the fluence of 4.74×10^{18} nvt (> 1 MeV) for iron dosimeters is equivalent to a maximum pressure vessel wall exposure of 1.90×10^{18} nvt (> 1 MeV). The surveillance capsule was removed after 0.844×10^6 Mw(t)-days of operation. The predicted fluence of the surveillance capsule based on the Technical Specification information is therefore only 5 percent greater than the measured fluence.

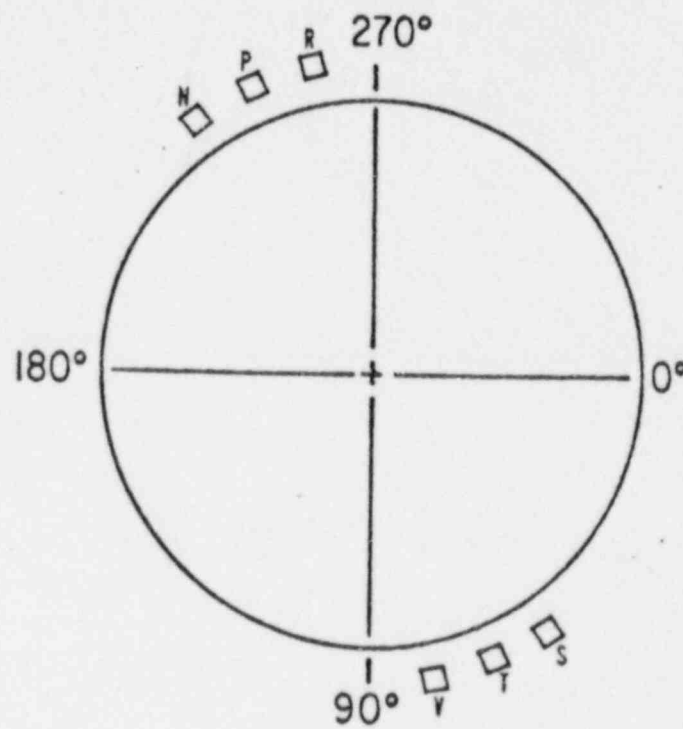


FIGURE 5. CAPSULE LOCATIONS IN REACTOR
Capsule V is at 77°.

TABLE 3. FAST NEUTRON DOSIMETRY RESULTS ($E > 1$ MeV)

Dosimeter	Location in Capsule	Fast Neutron ₂ Fluence, n/cm ²
Fe	Top	4.83×10^{18}
Fe	Mid-Top	4.59×10^{18}
Fe	Middle	4.46×10^{18}
Fe	Mid-Bottom	5.17×10^{18}
Fe	Bottom	4.62×10^{18}
	Avg	4.74×10^{18}
Cu	Top	4.76×10^{18}
Cu	Mid-Top	4.48×10^{18}
Cu	Mid-Bottom	4.88×10^{18}
Cu	Bottom	4.94×10^{18}
	Avg	4.76×10^{18}
Ni	Middle	3.80×10^{18}
U	Middle	8.24×10^{18}
Np	Middle	7.79×10^{18}

The thermal neutron fluences for the bare and cadmium covered cobalt dosimeters are shown in Table 4. The true thermal fluence was equal to 5.60×10^{18} n/cm², calculated from $nvt_{\text{true}} = Co_{\text{bare}} \times \frac{R-1}{R}$ where R (cadmium ratio) = $Co_{\text{bare}}/Co_{\text{Cd covered}} = 2.16$.

Basic counting data from fast and thermal monitors is shown in Appendix C.

Constants used in the calculations are summarized in Table 5 where the effective cross sections, σ_R , are of prime importance. The neutron flux and reaction cross section are defined in terms of the "fast flux" or neutron flux above 1.0 MeV as

$$\bar{\phi} \int_0^{\infty} \sigma(E)N(E)dE = \phi_f \frac{\int_0^{\infty} \sigma(E)N(E)dE}{\int_{1.0 \text{ MeV}}^{\infty} N(E)dE} = \phi_f \sigma_R, \quad (1)$$

where

$\bar{\phi}$ = neutron flux at full reactor power, n/cm²/sec

$\phi_f = \int_{1.0 \text{ MeV}}^{\infty} N(E)dE$ = flux above 1.0 MeV

σ_R = average reaction cross section above 1.0 MeV

$\sigma(E)$ = reaction cross section, cm², at energy E.

Calculations have been performed to determine the reaction cross sections, σ_R , and the activation correction factors, C, for five dosimeters placed in the reactor. The ANISN computer program was used to calculate the neutron energy spectrum at the dosimeter positions and to perform the integrations indicated in Equation (1). The dosimeter activation at the time of removal from the reactor is then

$$A = n \phi_f \sigma_R C,$$

where

A = disintegrations/cm³/sec

n = dosimeter nuclei concentrations, atoms/cm³.

TABLE 4. THERMAL NEUTRON DOSIMETRY RESULTS

Dosimeter	Location in Capsule	Fluence, ⁽¹⁾ n/cm ²
Co _{Bare}	Top	11.8×10^{18}
	Mid-Top	10.6×10^{18}
	Middle	8.55×10^{18}
	Mid-Bottom	10.4×10^{18}
	Bottom	10.6×10^{18}
	Avg.	10.4×10^{18}
Co _{Cadmium Covered}	Top	5.28×10^{18}
	Mid-Top	4.96×10^{18}
	Middle	4.38×10^{18}
	Mid-Bottom	4.96×10^{18}
	Bottom	4.55×10^{18}
	Avg	4.82×10^{18}
Average True Thermal ⁽²⁾		5.60×10^{18}

(1) These values show observed values not corrected for resonance energies.

(2) Corrected by factor $(R-1)/R$ where $R = Co_{Bare}/Co_{Cadmium} = 2.16$.

TABLE 5. VALUES USED IN DOSIMETRY CALCULATIONS

Reaction	Target	Target Isotope % Abundance	$\sigma^{(1)}$, R barns	Threshold Energy MeV	Fission Yield %	Product Half- Life
$^{63}\text{Cu}(n,\alpha)^{60}\text{Co}$	100% Cu	69.17	0.000608	5	--	5.26y
$^{58}\text{Ni}(n,p)^{58}\text{Co}$	100% Ni	67.77	0.105	1.0	--	71.3d
$^{54}\text{Fe}(n,p)^{54}\text{Mn}$	96.9% Iron	5.82	0.0785	1.5	--	314d
$^{238}\text{U}(n,f)^{137}\text{Cs}$	U_3O_8	>99.9	0.345	0.8	6.2	30.0y
$^{237}\text{Np}(n,f)^{137}\text{Cs}$	NpO_2	>99.9	2.66	0.4	6.0	30.0y
$^{59}\text{Co}(n,\gamma)^{60}\text{Co}$	Al-0.15% Co	100	37.1	--	--	5.26y

(1) For fast reactions, σ_R is for neutrons >1 MeV at capsule location.

$$C = \sum_{j=1}^J F_j (1 - e^{-\lambda \tau_j}) e^{-\lambda(T - t_j)} = \text{activation correction factor,}$$

t_j = the elapsed time at the end of the j^{th} time interval, sec

J = number of time intervals

F_j = fractional power level during a time interval τ_j

λ = dosimeter decay constant, sec^{-1}

T = length of time the dosimeter is in the reactor, sec.

Figure 6 is a comparison of the ANISN-calculated neutron spectrum with the fission spectrum. It is seen that the ANISN spectrum contains far fewer high-energy neutrons than the fission spectrum. At the dosimeter location the ratio of the fast flux above 1.0 MeV to the total flux

$$\frac{\phi_F}{\phi} = 0.0426.$$

This causes the ANISN-calculated values of σ_R to be considerably smaller than the fission-spectrum-averaged cross sections. The activation correction factors were calculated for Point Beach Unit No. 2 operation through October 31, 1974. The power history was taken from Reference (22). The decay for the Np^{237} and U^{238} dosimeters was calculated for the fission product Cs-137.

Appendix D contains a letter from Westinghouse to Wisconsin Electric containing dosimeter and capsule information. This information includes dosimeter material purities, capsule location in the reactor, and capsule exposure lead factor.

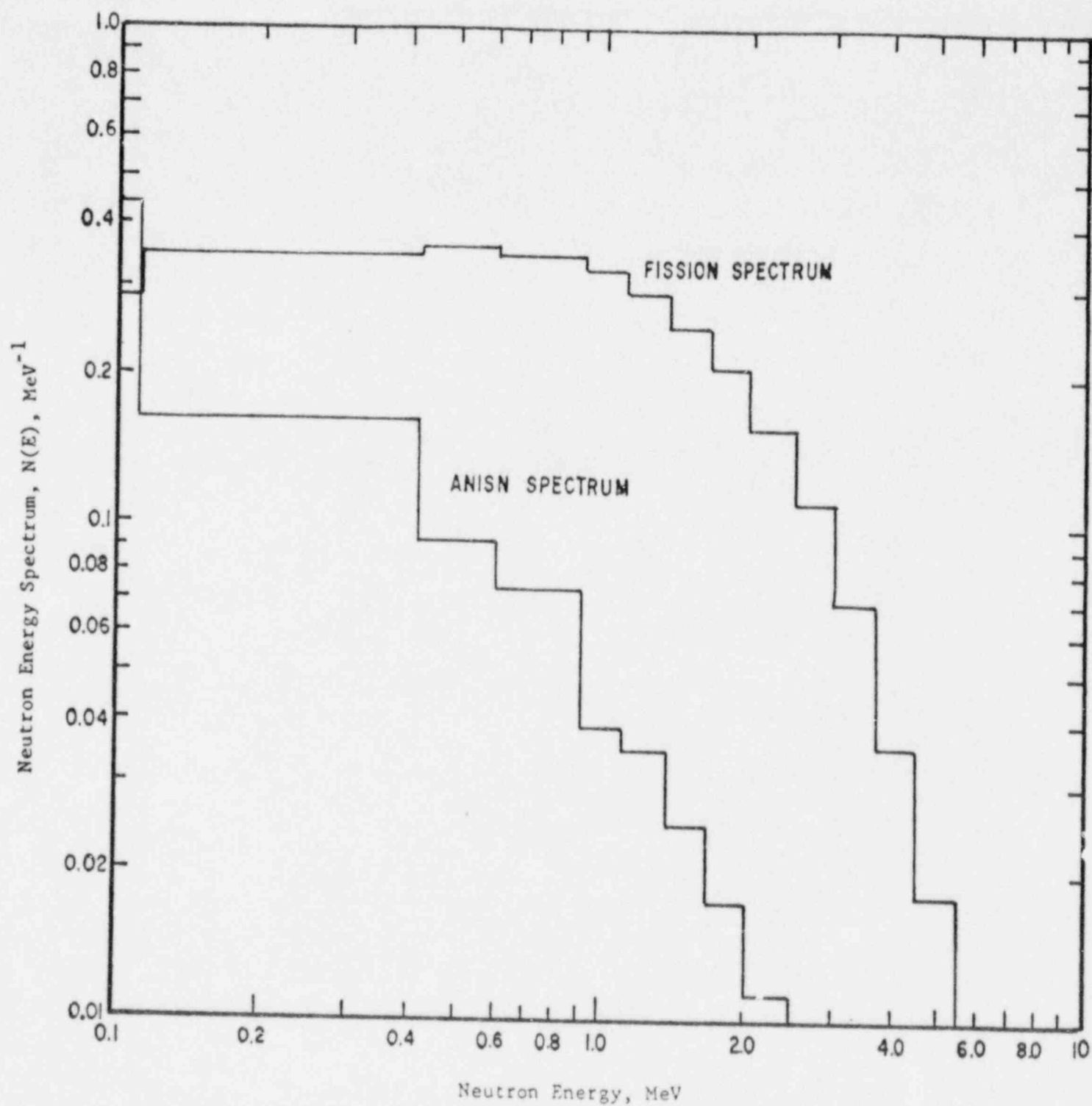


FIGURE 6. COMPARISON OF THE NEUTRON FISSION SPECTRUM WITH THE ANISN-CALCULATED SPECTRUM AT THE DOSIMETER LOCATION FOR POINT BEACH UNIT NO. 2

Tensile Properties

The irradiated tensile properties are listed in Table 6A for the base and weld metal. The table lists temperature, 0.2 percent offset yield strength, ultimate tensile strength, fracture stress, fracture strength, uniform elongation, total elongation, and reduction in area. The unirradiated tensile properties from Reference (9) are listed in Table 6B for comparison. Posttest photographs at 4X of the tensile specimens are shown in Figures 7 through 9. These photographs show the necked down region of the gage length and the fracture. A typical tensile curve showing stress as a function of strain is shown in Figure 10; the particular test shown is for base metal specimen V1 tested at 550 F.

Tensile tests for the irradiated metals were run at room temperature, 300, and 550 F. The results are shown compared to the unirradiated properties from Reference (9) in Figures 11, 12, and 13, which are plots of ultimate tensile strength, 0.2 percent offset yield strength, reduction in area, and total elongation. The yield strengths and ultimate tensile strengths increased after irradiation for all three metals at the three temperatures except for the two base metals at 300 F. The reduction in area after irradiation was the same or slightly less than before irradiation for the two base metals, but decreased appreciably after irradiation for the weld metal. The total elongation after irradiation for the base metal 122W195VA1 decreased slightly at 88 and 550 F, but was unchanged at 300 F. The total elongation after irradiation for the base metal plate 123V500VA1 and the weld metal decreased at all three test temperatures, with the weld metal showing the greater decreases.

TABLE 6A. POINT BEACH UNIT NO. 2 IRRADIATED TENSILE PROPERTIES

Material	Specimen	Temp., F	0.2% Offset Yield Strength, psi	Ultimate Tensile Strength, psi	Fracture Strength, psi	Fracture Stress, psi	Uniform Elongation, %	Total Elongation, %	Reduction in Area, %
Base (122W195VA1)	E2	88	75,300	97,400	60,410	189,740	9.2	21.5	68.1
Base (122W195VA1)	E3	300	66,400	89,200	56,620	180,520	8.6	20.4	68.6
Base (122W195VA1)	E1	550	74,900	100,200	64,290	199,370	8.3	19.6	67.8
Base (123V500VA1)	V2	88	67,700	91,200	54,990	191,490	10.5	23.2	71.3
Base (123V500VA1)	V3	300	57,400	80,700	51,120	172,410	10.1	22.3	70.3
Base (123V500VA1)	V1	550	74,100	96,800	61,220	192,310	9.1	20.9	68.1
Weld	W2	88	88,600	105,800	78,820	176,710	11.2	21.0	53.4
Weld	W3	300	80,200	97,100	77,100	123,200	9.7	17.6	37.4
Weld	W1	550	81,200	99,700	82,820	148,900	7.3	16.3	44.4

TABLE 6B. PREIRRADIATION TENSILE PROPERTIES FOR THE
POINT BEACH UNIT NO. 2 REACTOR PRESSURE
VESSEL SHELL FORGINGS AND WELD METAL (a)

Shell Forging Material	Test Temp. (F)	0.2% Yield Strength (psi)	Ultimate Tensile Strength (psi)	Uniform Elong. (%)	Total Elong. (%)	Reduction in Area (%)
123V500VA1	Room	57,050	82,100	17.2	32.0	72.7
	Room	53,800	78,400	18.1	31.9	72.3
	300	63,450	84,500	13.3	25.5	73.4
	300	55,500	78,400	15.1	25.5	68.0
	600	44,500	77,300	14.4	27.9	72.3
	600	49,700	78,950	16.5	28.5	71.1
122W195VA1	Room	71,100	92,500	14.1	27.5	70.5
	Room	70,500	91,450	13.9	26.6	70.5
	300	71,500	92,150	10.4	21.6	72.3
	300	64,500	85,550	11.0	22.2	69.6
	600	64,350	90,650	13.9	27.2	72.3
	600	61,600	86,800	14.2	28.1	71.9
Weld Metal	Room	71,300	86,150	16.4	27.2	64.1
	Room	72,500	87,800	15.9	27.0	64.1
	300	66,800	82,000	11.4	22.8	63.1
	300	64,600	79,550	13.9	24.0	64.1
	600	63,750	85,750	13.7	21.9	54.6
	600	62,500	84,000	15.6	23.9	54.6

(a) This tensile data is from Reference (9).

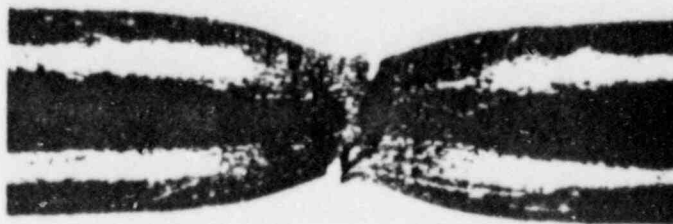


FIGURE 7a. TENSILE SPECIMEN E2 TESTED AT 88 F

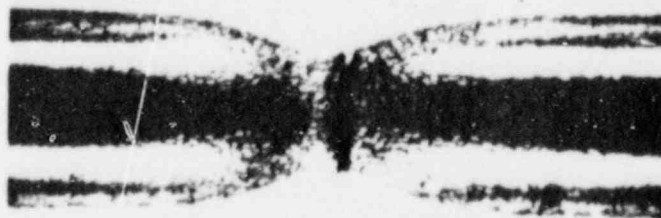


FIGURE 7b. TENSILE SPECIMEN E3 TESTED AT 300 F

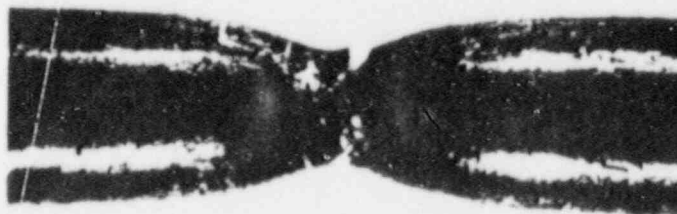


FIGURE 7c. TENSILE SPECIMEN E1 TESTED AT 550 F



FIGURE 8a. TENSILE SPECIMEN V2 TESTED AT 88 F



FIGURE 8b. TENSILE SPECIMEN V3 TESTED AT 300 F



FIGURE 8c. TENSILE SPECIMEN V1 TESTED AT 550 F



FIGURE 9a. TENSILE SPECIMEN W2 TESTED AT 88 F

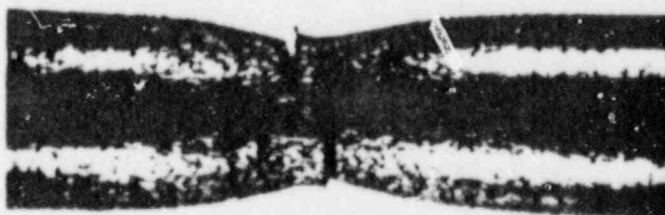


FIGURE 9b. TENSILE SPECIMEN W3 TESTED AT 300 F



FIGURE 9c. TENSILE SPECIMEN W1 TESTED AT 550 F

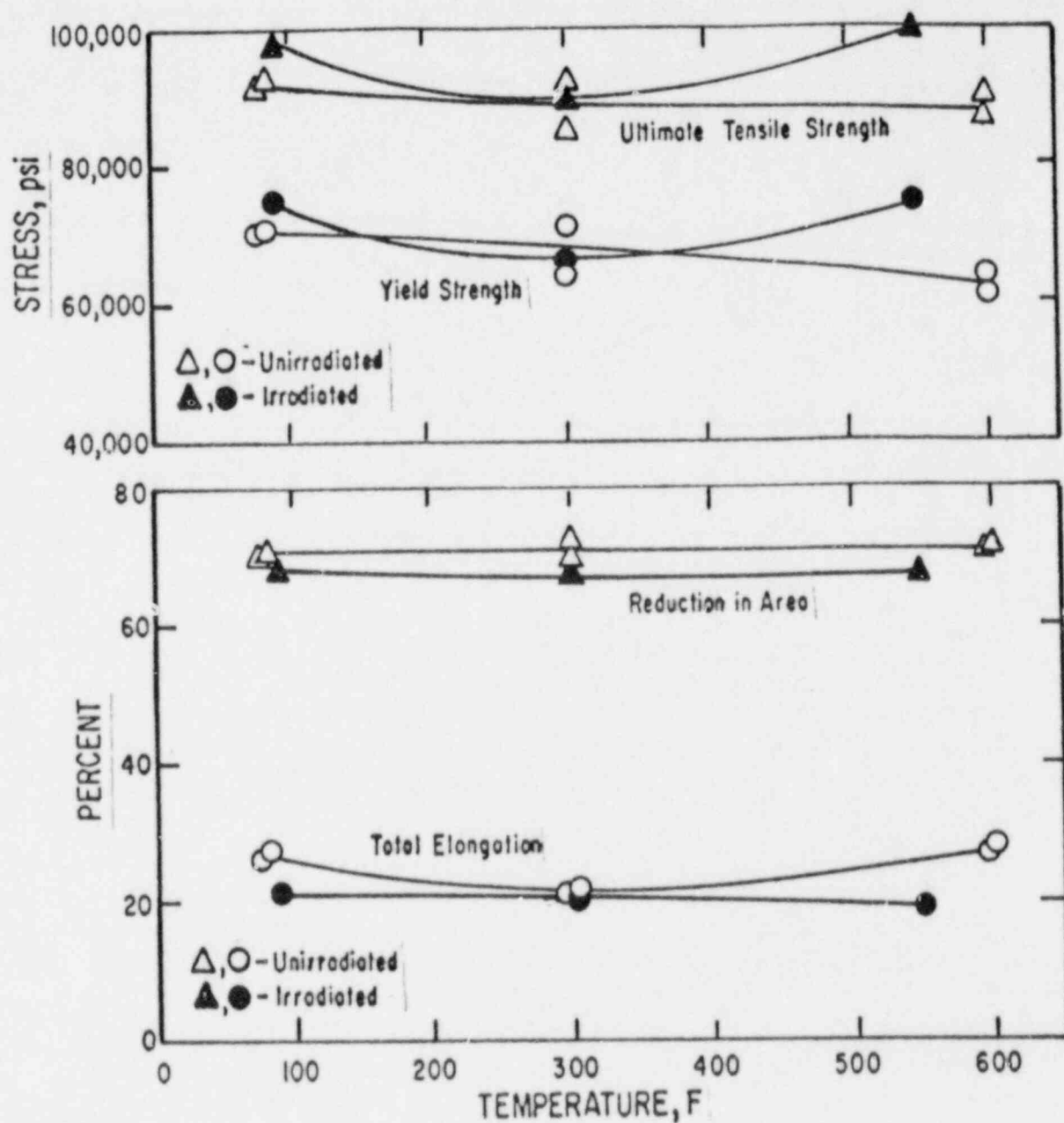


FIGURE 11. COMPARISON OF UNIRRADIATED AND IRRADIATED TENSILE PROPERTIES FOR POINT BEACH UNIT NO. 2 BASE METAL PLATE 122W195VA1

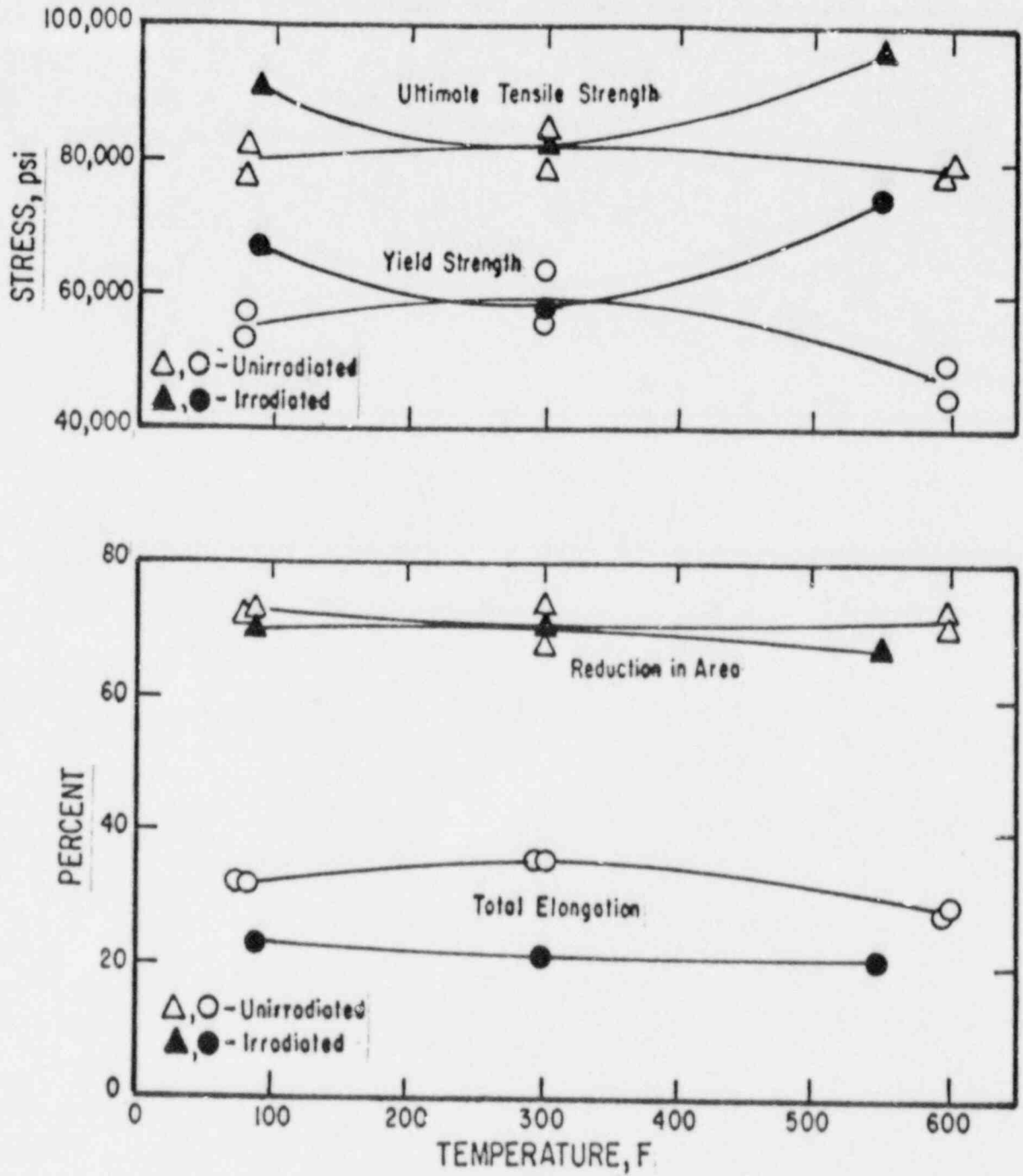


FIGURE 12. COMPARISON OF UNIRRADIATED AND IRRADIATED TENSILE PROPERTIES FOR POINT BEACH UNIT NO. 2 BASE METAL PLATE 123V500VA1

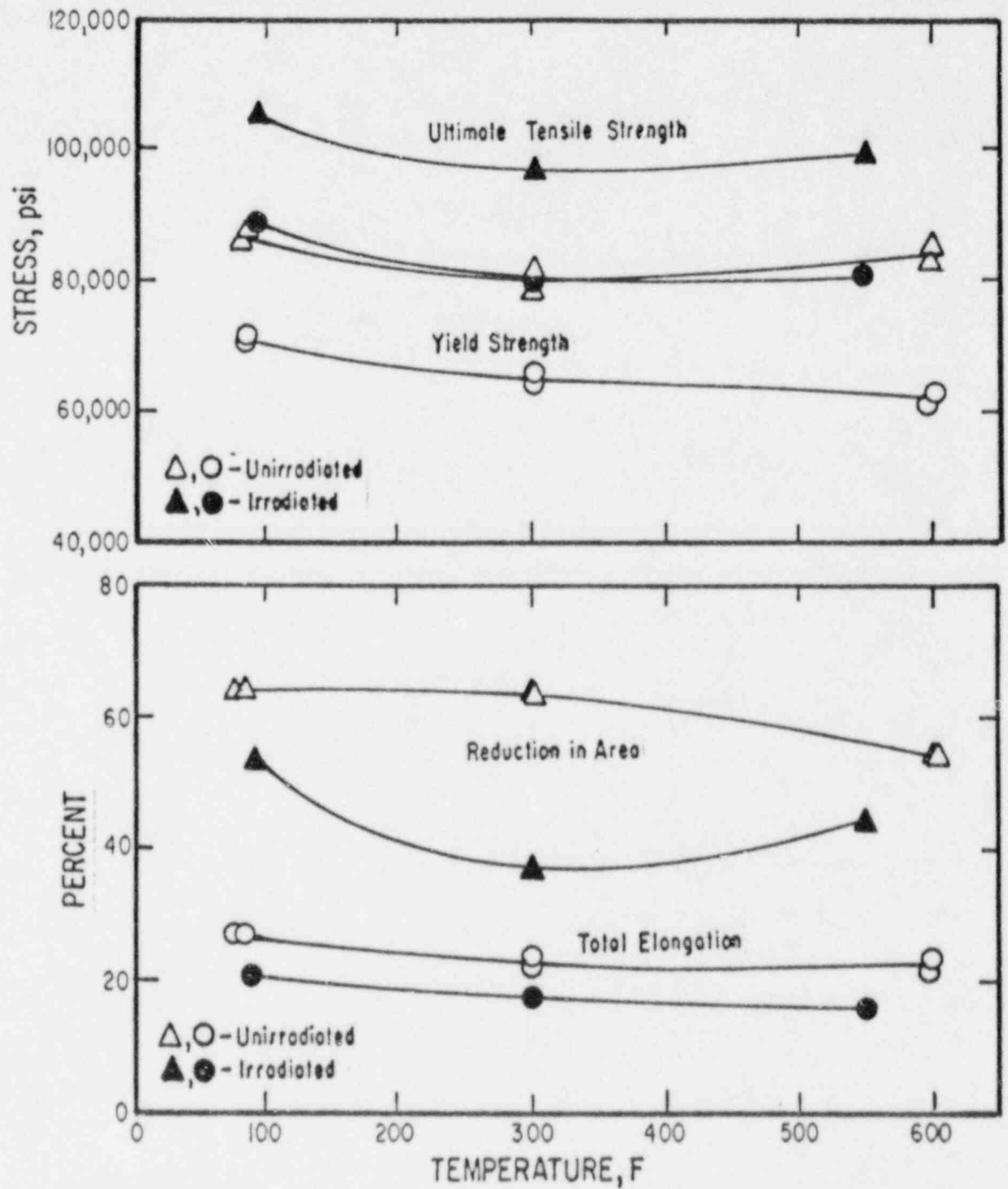


FIGURE 13. COMPARISON OF UNIRRADIATED AND IRRADIATED TENSILE PROPERTIES FOR POINT BEACH UNIT NO. 2 WELD METAL

Charpy Impact Properties

The impact properties determined as a function of temperature are listed in Tables 7 through 11. In addition to the impact energy values, the tables also list the measured values of lateral expansion and the estimated fracture appearance for each specimen. The lateral expansion is a measure of the deformation produced by the striking edge of the impact machine hammer when it impacts the specimen; it is the change in specimen thickness of the section directly adjacent to the notch location. The fracture appearance is a visual estimate of the amount of shear or ductile type of fracture appearing on the specimen fracture surface.

The impact data listed in Tables 7 through 11 are graphically shown in Figures 14 through 18. These figures show the change in impact properties as a function of temperature. The data for the irradiated curves was determined in the present program, and the unirradiated curves are from WCAP 7712⁽⁹⁾. Of particular interest are the temperatures corresponding to the impact energies of 30 and 50 ft-lb. The energy level of the upper shelf is also of interest.

The curves for the five irradiated metals are well defined with little data scatter with only one exception. The exception is the curve for the irradiated HAZ metal. The reason for this is that it is difficult to cut specimens out of a heat affected zone in a plate between base metal and weld metal, and be assured that the HAZ specimens all have the identical microstructure and thermal history. The unirradiated impact data for the HAZ metal also showed substantial data scatter.

TABLE 7. CHARPY V-NOTCH IMPACT TEST RESULTS FOR
BASE METAL PLATE 122W195VA1 (E SERIES)

Specimen	Test Temperature, F	Impact Energy, ft-lb	Lateral Expansion, mils	Fracture Appearance, Percent Shear
E1	-80	5.0	8.0	5
E3	-80	7.5	11.5	2
E8	-45	25.5	25.5	10
E2	0	58.5	46.0	30
E4	0	10.5	18.0	5
E9	0	55.0	47.0	25
E7	74	86.0	66.5	100
E11	76	76.5	67.0	55
E5	145	141.5	98.5	100
E6	145	133.0	90.0	100
E12	200	136.5	89.5	100
E10	290	135.0	88.0	100

TABLE 8. CHARPY V-NOTCH IMPACT TEST RESULTS FOR
BASE METAL PLATE 123V500VA1 (V SERIES)

Specimen	Test Temperature, F	Impact Energy, ft-lb	Lateral Expansion, mils	Fracture Appearance, Percent Shear
V10	-80	3.5	11.0	0
V3	-80	2.0	6.5	0
V6	-45	50.5	48.0	15
V1	-45	22.0	29.5	5
V2	0	90.0	80.0	50
V11	0	94.5	90.5	50
V12	74	114.5	89.5	65
V7	76	108.5	75.5	65
V5	145	186.5	87.5	100
V4	200	216.0	72.5	100
V9	290	165.0	78.5	100
V8	345	198.5	75.5	100

TABLE 9. CHARPY V-NOTCH IMPACT TEST RESULTS
FOR WELD METAL

Specimen	Test Temperature, F	Impact Energy, ft-lb	Lateral Expansion, mils	Fracture Appearance, Percent Shear
W6	76	13.5	15.5	7
W3	145	22.5	26.5	35
W5	145	27.0	31.5	40
W8	200	43.0	46.8	90
W1	290	41.5	48.0	100
W7	310	41.0	45.5	100
W2	345	41.5	52.5	100
W4	345	43.5	47.0	100

TABLE 10. CHARPY V-NOTCH IMPACT TEST RESULTS FOR
HEAT AFFECTED ZONE METAL

Specimen	Test Temperature, F	Impact Energy, ft-lb	Lateral Expansion, mils	Fracture Appearance, Percent Shear
H2	0	10.5	14.0	2
H5	0	27.0	31.0	15
H8	0	15.0	15.5	2
H1	76	115.0	82.0	90
H6	76	152.0	67.5	100
H4	145	177.0	91.5	100
H7	200	102.5	75.5	60
H3	290	195.0	91.0	100

TABLE 11. CHARPY V-NOTCH IMPACT TEST RESULTS FOR
ASTM CORRELATION MONITOR METAL

Specimen	Test Temperature, F	Impact Energy, ft-lb	Lateral Expansion, mils	Fracture Appearance, Percent Shear
R7	76	9.5	13.5	10
R2	80	7.0	11.0	10
R4	145	39.0	43.5	25
R5	145	31.0	35.5	30
R6	200	55.0	54.5	50
R8	290	81.5	75.5	90
R1	345	96.5	83.5	100
R3	345	90.5	88.0	100

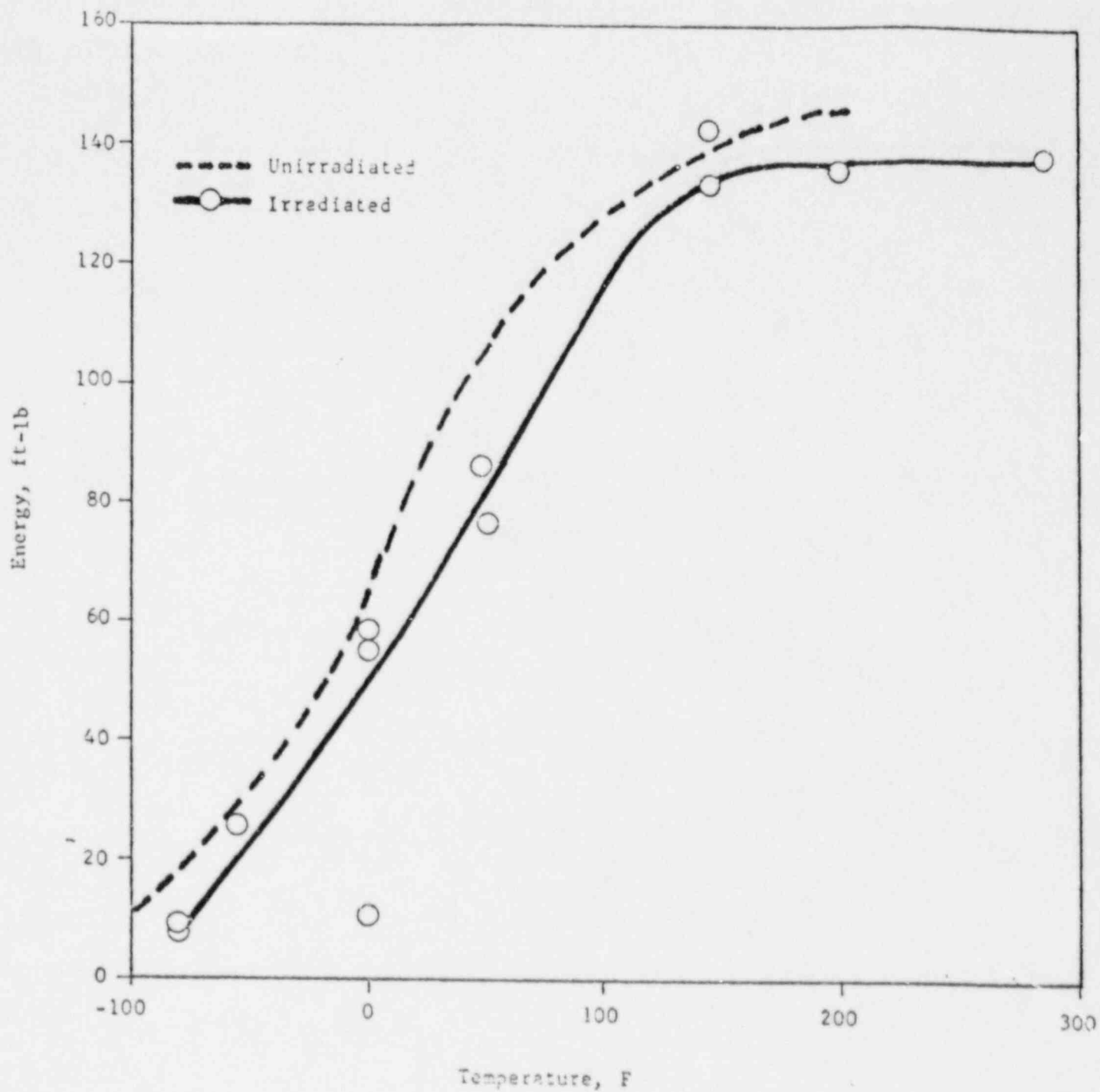


FIGURE 14. CHARPY IMPACT ENERGY VERSUS TEMPERATURE FOR POINT BEACH UNIT NO. 2 BASE METAL (122W193VA1)

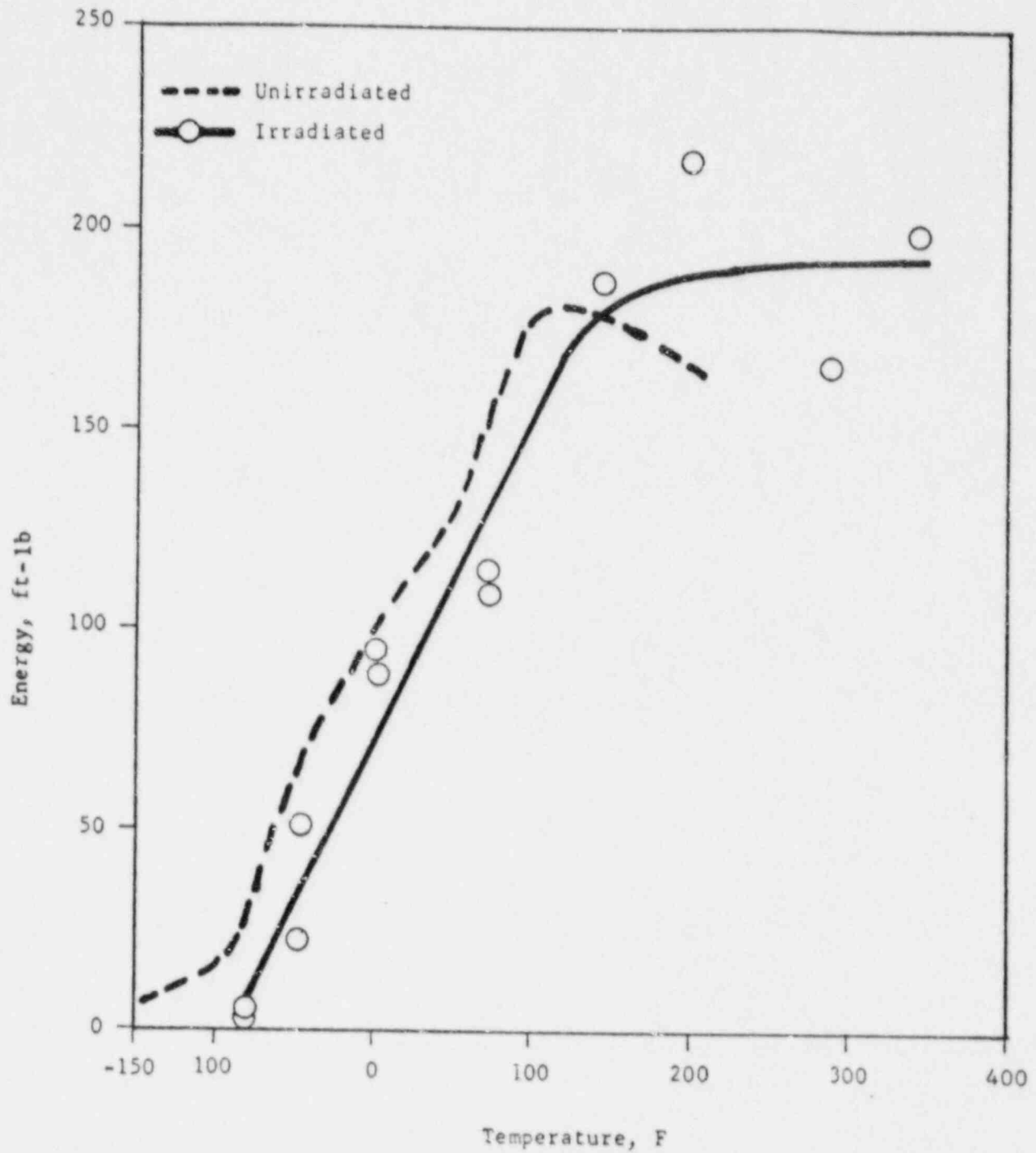


FIGURE 15. CHARPY IMPACT ENERGY VERSUS TEMPERATURE FOR
POINT BEACH UNIT NO. 2 BASE METAL (123V500VA1)

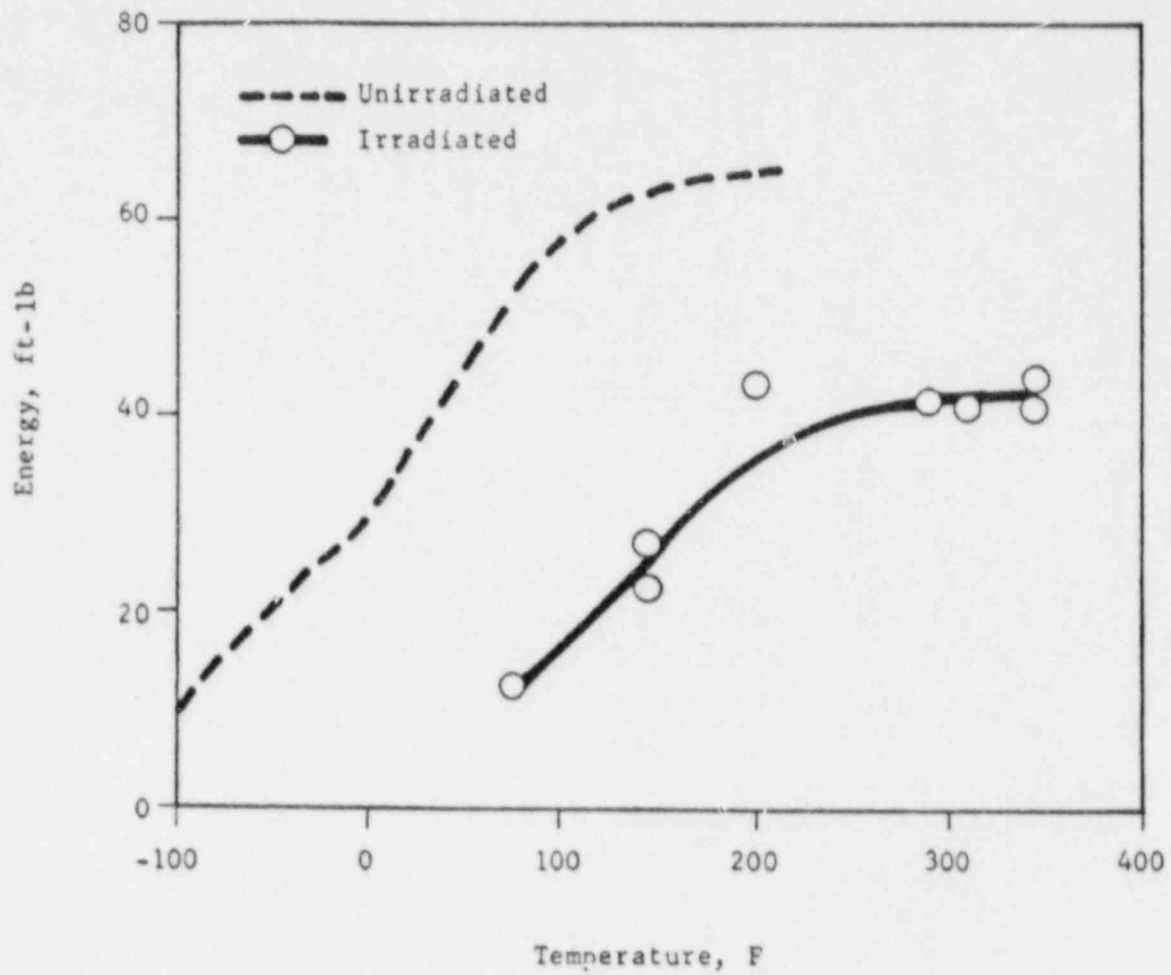


FIGURE 16. CHARPY IMPACT ENERGY VERSUS TEMPERATURE FOR
POINT BEACH UNIT NO. 2 WELD METAL

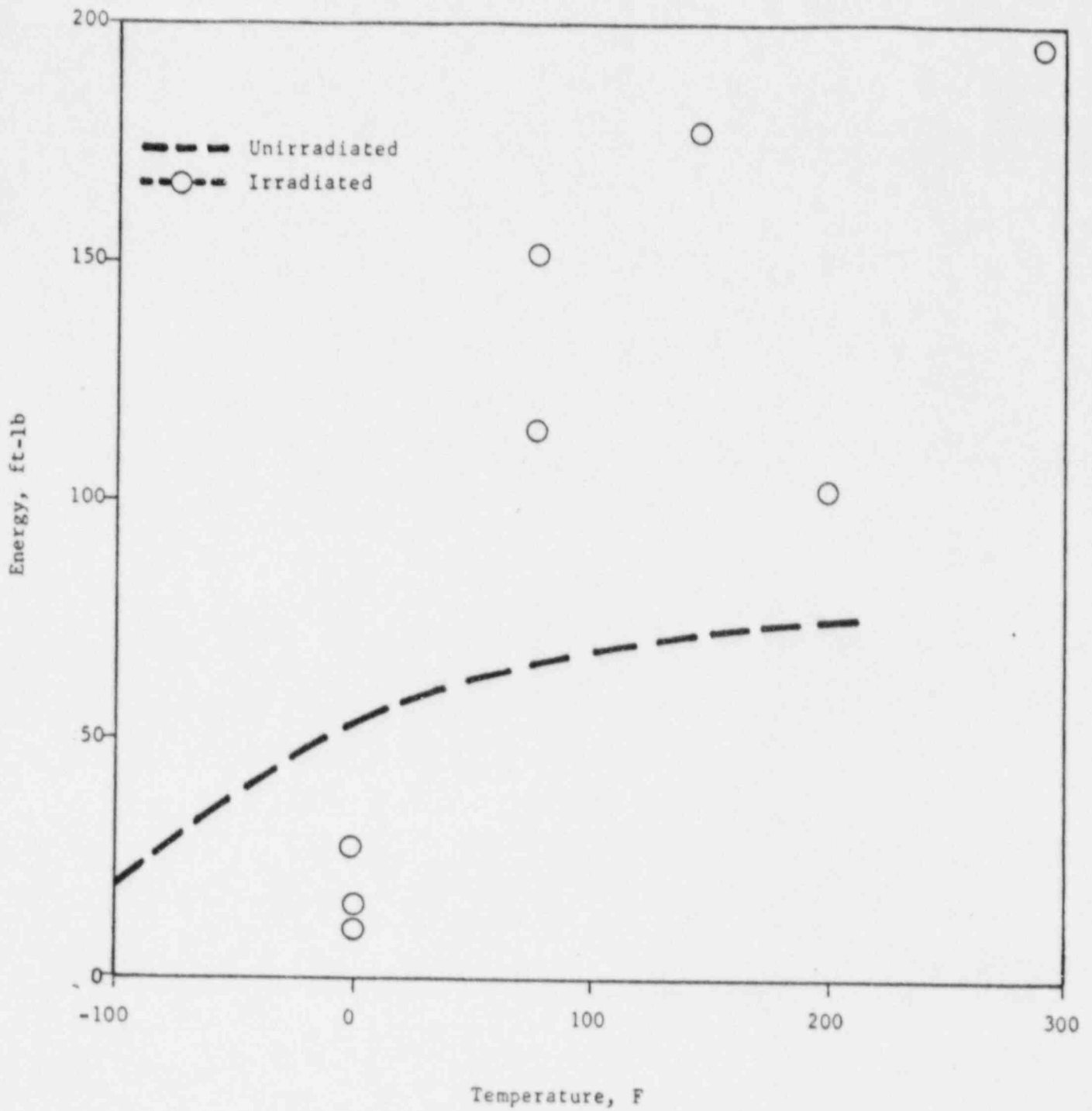


FIGURE 17. CHARPY IMPACT ENERGY VERSUS TEMPERATURE FOR POINT BEACH UNIT NO. 2 HAZ METAL

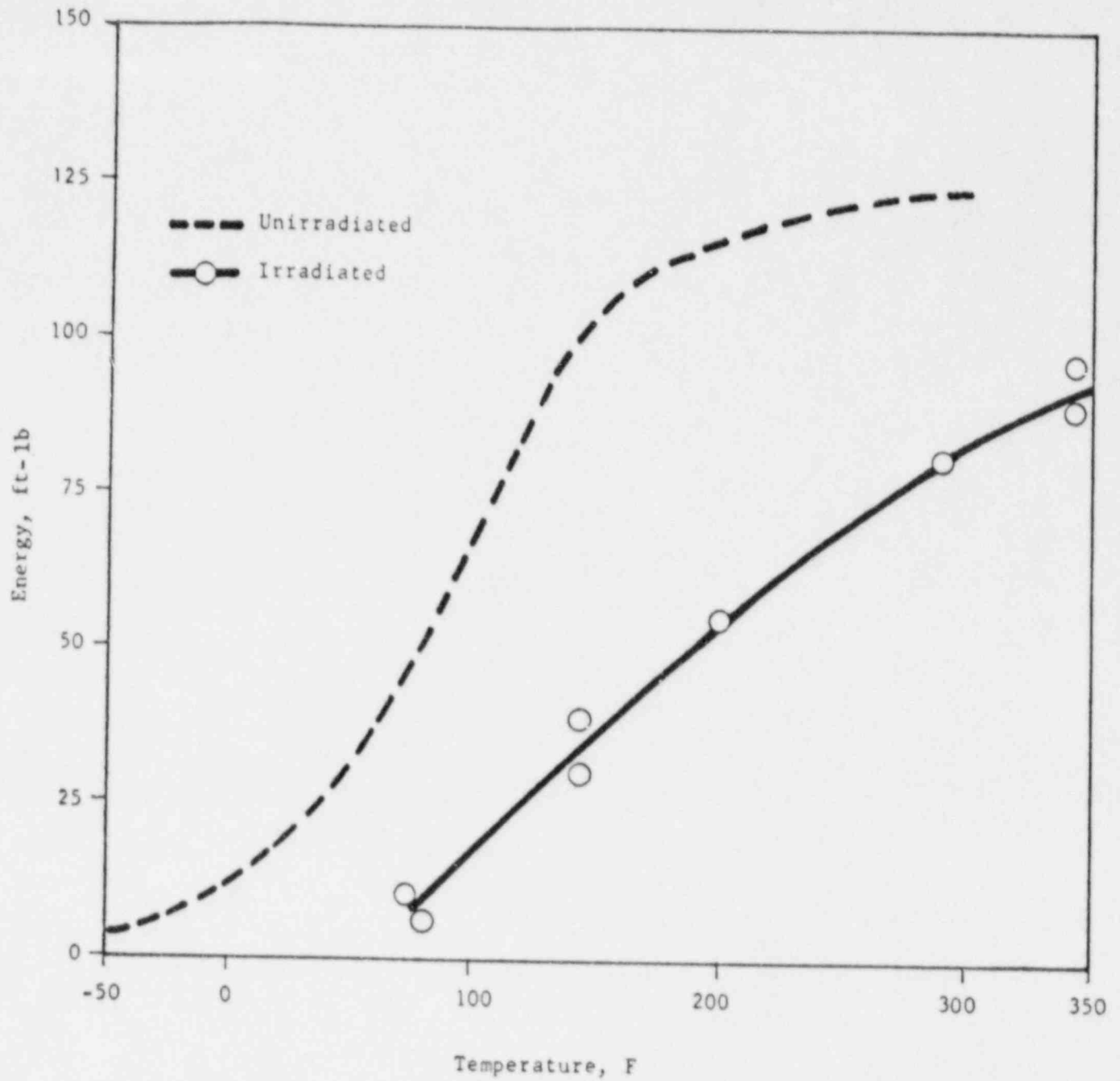


FIGURE 18. CHARPY IMPACT ENERGY VERSUS TEMPERATURE FOR POINT BEACH
UNIT NO. 2 ASTM CORRELATION MONITOR METAL

Figures 19 through 23 show the fracture surfaces of the Charpy specimens. Figure 19, as an example, shows how the fracture surface changes as the test temperature is increased for base metal specimens. The -80 F specimen (E1) shows an almost flat fracture surface, with only 5 percent shear fracture appearance. This specimen absorbed 8.0 ft-lb of energy during the impact test, a typically low value for the low temperature, brittle region of the Charpy curve. As can be seen in the figure, the amount of lateral expansion is small, and was measured as being only 8.0 mils. As the test temperature is increased, specimens show an increasing amount of shear fracture appearance. The +290 F specimen (E10) fracture surface is typical of the type seen at the higher temperature end of the Charpy transition curve. The fracture surface shows large shear lips with a 100% shear fracture appearance. The specimen absorbed the relatively large amount of 135.0 ft-lb during impact. The substantial amount of plastic deformation occurring during this test is reflected in the large value of 88.0 mils lateral expansion.

Table 12 summarizes the unirradiated and irradiated 30 and 50 ft-lb transition temperatures and the upper shelf energy levels for the five metals. Table 13 lists the 30 ft-lb and 50 ft-lb transition temperature shifts due to irradiation. The 30 and 50 ft-lb transition temperatures are difficult to determine for the HAZ metal due to the scatter in the data.

The ASTM correlation monitor metal shows a 30 ft-lb shift of 90 F and a 50 ft-lb shift of 110 ft-lb. Irradiation has caused the upper shelf energy to drop from 125 to 95 ft-lb.

For the four reactor vessel metals, the irradiated 30 ft-lb transition temperature ranges from -50 F (base) to 165 F (weld). The HAZ value is difficult to define due to data scatter, but is below the 165 F weld metal value. The largest shift due to irradiation is an increase from 0 F to 165 F, a total of 165 F, for the weld metal. The irradiated 50 ft-lb transition temperature ranges from -25 F (base) to an undefined value for the weld metal due to an upper shelf below 50 ft-lb. The 50 ft-lb HAZ value is difficult to define due to data scatter, but the most conservative curve through the data yields a value below 100 F.

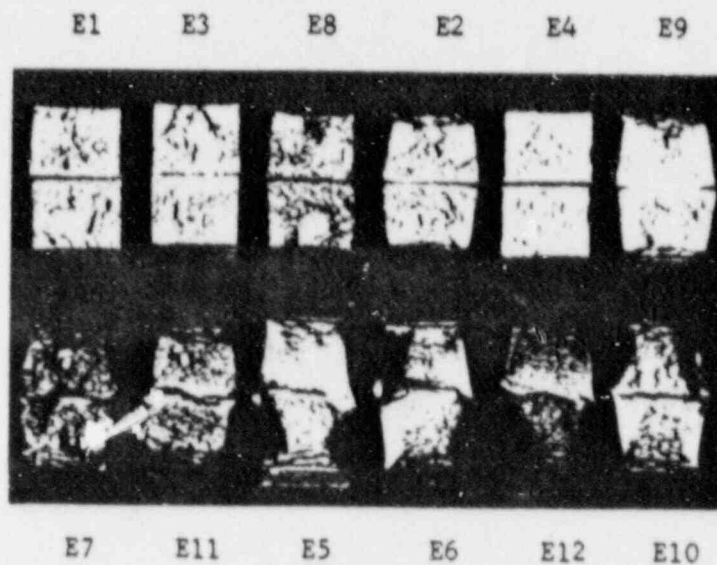


FIGURE 19. CHARPY IMPACT SPECIMEN FRACTURE SURFACES FOR
POINT BEACH UNIT NO. 2 BASE METAL PLATE
122W195VA1

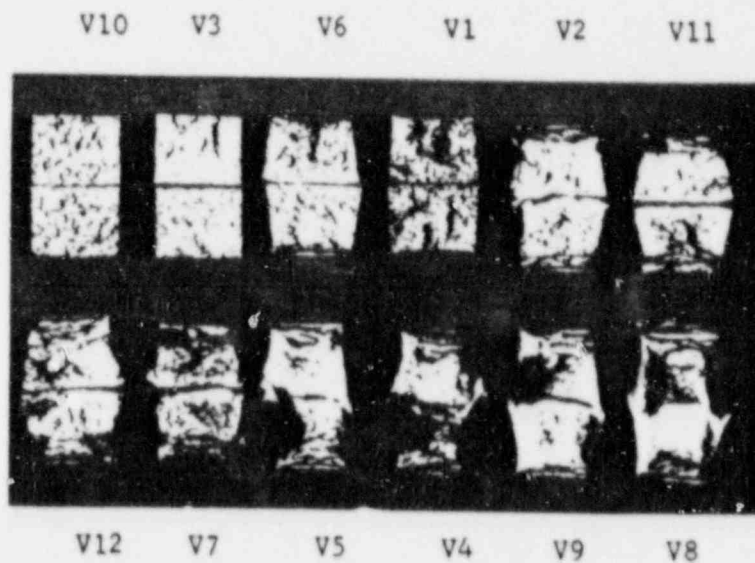


FIGURE 20. CHARPY IMPACT SPECIMEN FRACTURE SURFACES FOR
POINT BEACH UNIT NO. 2 BASE METAL PLATE
123V500VA1

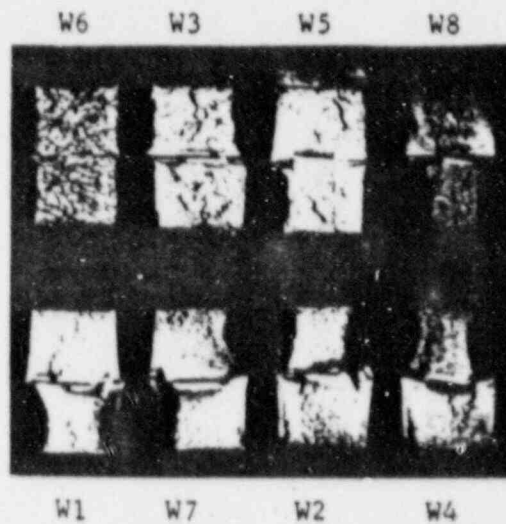


FIGURE 21. CHARPY IMPACT SPECIMEN FRACTURE SURFACES FOR
POINT BEACH UNIT NO. 2 WELD METAL

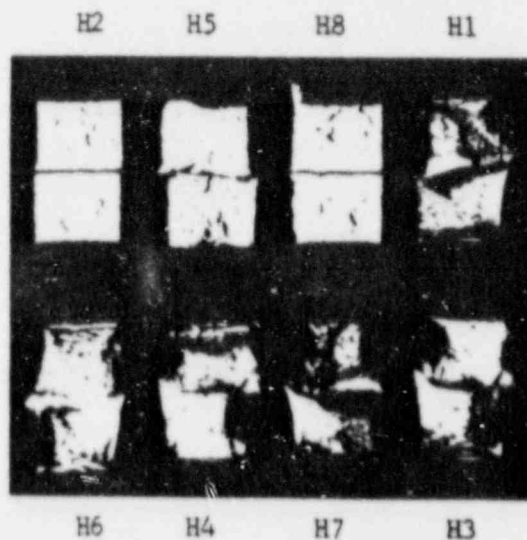


FIGURE 22. CHARPY IMPACT SPECIMEN FRACTURE SURFACES FOR
POINT BEACH UNIT NO. 2 HAZ METAL

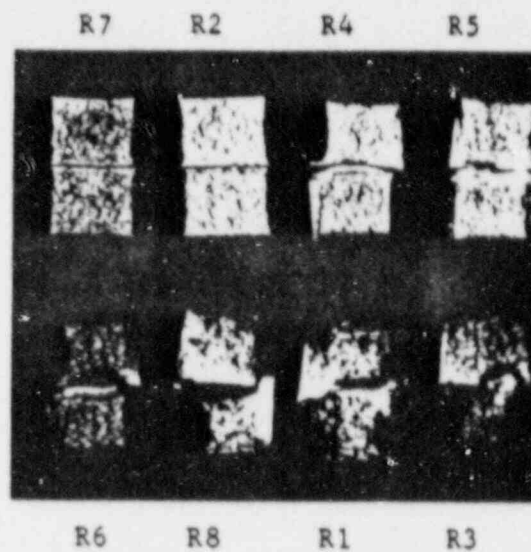


FIGURE 23. CHARPY IMPACT SPECIMEN FRACTURE SURFACES FOR
POINT BEACH UNIT NO. 2 ASTM CORRELATION
MONITOR METAL

TABLE 12. CHARPY IMPACT PROPERTIES FOR
POINT BEACH UNIT NO. 2

Material	Condition	Transition Temperature, F		Upper Shelf, ft-lb
		30 ft-lb	50 ft-lb	
Base (122W195VA1)	Unirradiated	-55	-15	145
Base (122W195VA1)	Irradiated	-35	0	135
Base (123V500VA1)	Unirradiated	-80	-60	180
Base (123V500VA1)	Irradiated	-50	-25	190
Weld	Unirradiated	0	60	65
Weld	Irradiated	165	--	42
HAZ	Unirradiated	(a)	(a)	(a)
HAZ	Irradiated	(a)	(a)	(a)
ASTM Correlation	Unirradiated	45	80	125
ASTM Correlation	Irradiated	135	190	95

(a) See text for discussion of HAZ metal.

TABLE 13. COMPARISON OF POINT BEACH UNIT NO. 2
30 FT-LB and 50 FT-LB TRANSITION
TEMPERATURE SHIFTS

Material	30 ft-lb Transition Temperature Shift,	50 ft-lb Transition Temperature Shift,
	F	F
Base (122W195VA1)	20	15
Base (123V500VA1)	30	35
Weld	165	--
HAZ	(a)	(a)
ASTM Correlation	90	110

(a) See text for discussion of HAZ metal.

One base metal upper shelf dropped from 145 to 135 ft-lb, a change of 10 ft-lb. The other base metal upper shelf shows an increase from 180 to 190 ft-lb; this apparent increase is probably due to data scatter because upper shelf energy levels normally decrease due to irradiation. The weld metal upper shelf dropped from 65 to 42 ft-lb, a change of 23 ft-lb. The upper shelf change for the HAZ metal is difficult to determine due to the large amount of data scatter.

The significant drop in upper shelf energy level for the weld metal from 65 ft-lb to the relatively low value of 42 ft-lb represents a decrease of 23 ft-lb or 35 percent. Drops of this magnitude have been associated with high residual element levels⁽²³⁾. The chemical compositions of the base metal and weld metal used for the surveillance capsule specimens is presented in Appendix A of this report. The weld metal copper content is quite high, having a value of 0.25 weight percent. It is this relatively high copper level which is most probably causing the low irradiated upper shelf level of the weld metal.

The transition temperature shifts for the three reactor vessel metals are shown plotted in Figures 24 and 25 as a function of fluence. The two figures are the 30 and 50 ft-lb transition temperature shift values obtained in the present surveillance program and in other surveillance programs for A302B and A508 pressure vessel steels⁽²⁴⁻³¹⁾. HAZ values from the present program are not included. Weld metal values from the present program are shown only in Figure 24, since only the 30 ft-lb value is defined. The values used to form the trend band are those from programs where the irradiation temperature was between 550 and 590 F. The apparent large scatter in data among the various programs is not unusual. Note that the weld metal values generally determine the upper bound of the trend band. It can be seen that the transition temperature shift values for the base metals of the present program fall within the upper and lower bounds determined by metals of the other programs. The weld metal 30 ft-lb value for the present program in Figure 24 falls above the trend band.

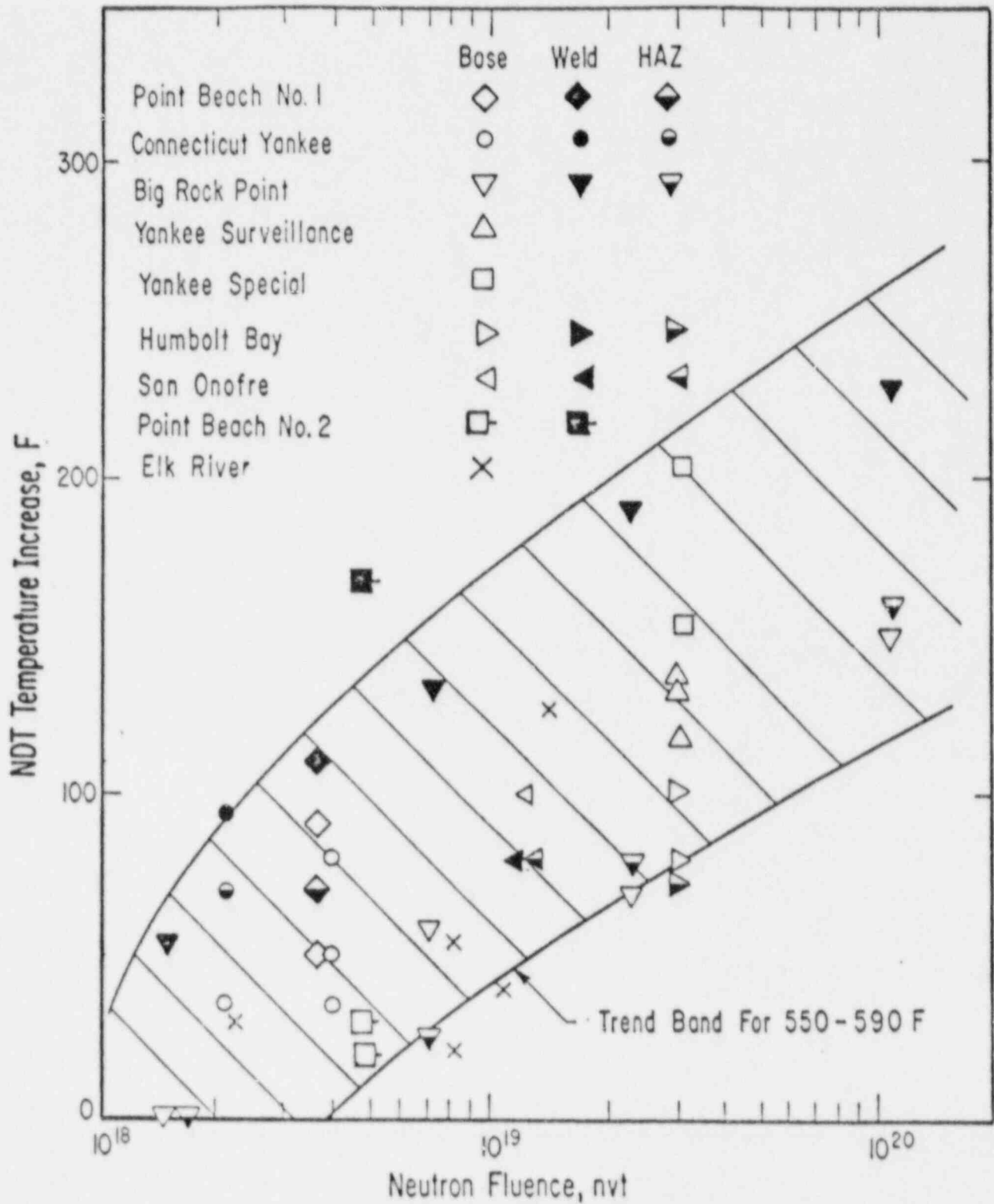


FIGURE 24. COMPARISON OF 30 FT-LB TRANSITION TEMPERATURE VALUES FROM VARIOUS SURVEILLANCE PROGRAMS FOR A302 GRADE B AND A508 PRESSURE VESSEL STEELS

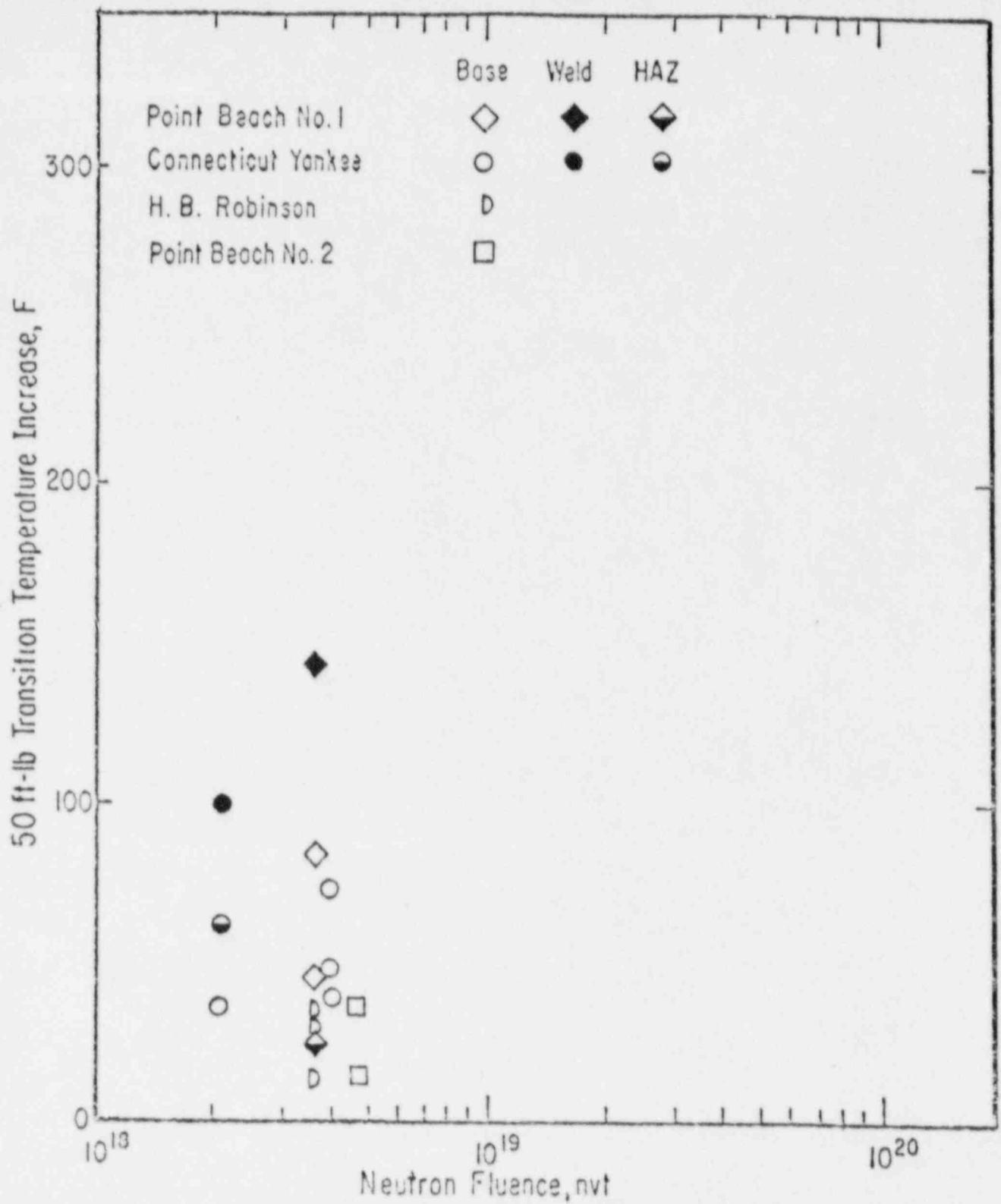


FIGURE 25. COMPARISON OF 50 FT-LB TRANSITION TEMPERATURE VALUES FROM VARIOUS SURVEILLANCE PROGRAMS FOR A302 GRAD B AND A508 PRESSURE VESSEL STEELS

The 30 ft-lb transition temperature value for the ASTM correlation monitor material is shown in Figure 26. Also shown in this figure are the 30 ft-lb transition temperature values obtained from other programs using ASTM correlation monitor A302 and A533 pressure vessel steels. The 30 ft-lb transition temperature value determined in the present program for ASTM A533 correlation monitor material is consistent with other values shown.

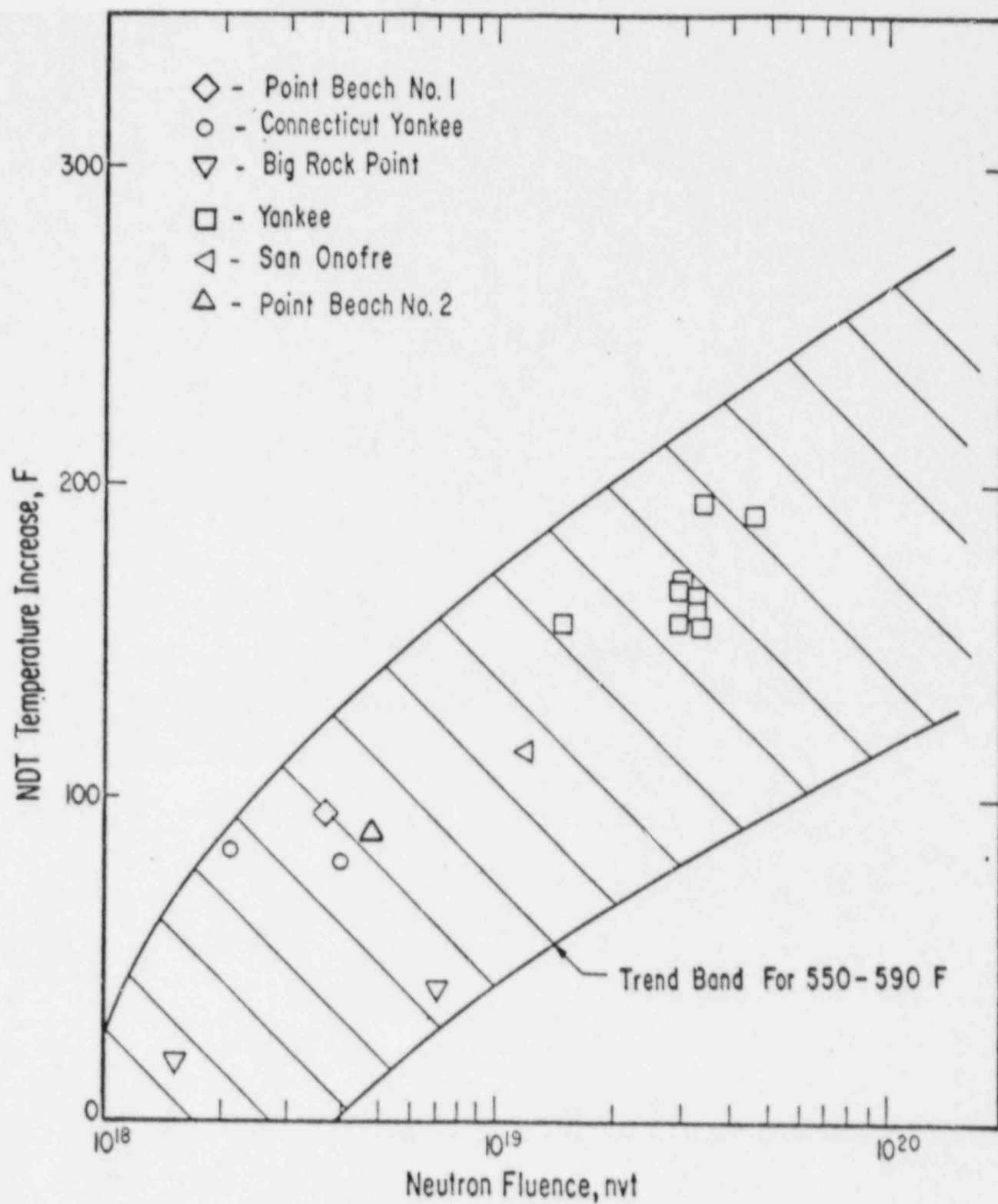


FIGURE 26. COMPARISON OF 30 FT-LB VALUES FROM VARIOUS SURVEILLANCE PROGRAMS FOR ASTM CORRELATION-MONITOR STEELS

CONCLUSIONS

The maximum irradiation temperature of the irradiation surveillance capsule did not exceed 590 F. The neutron fluence experienced by the capsule was 4.74×10^{18} nvt (>1 MeV) which was attained after 1.52 equivalent full-power years of operation. Based on a capsule lead factor of 2.5, this is equivalent to a maximum fluence of 1.90×10^{18} nvt (>1 MeV) for the pressure vessel after 1.52 equivalent full power years. For a pressure vessel life of 40 years operation at an 80 percent load factor (32 equivalent full power years), the maximum fluence experienced by the pressure vessel would therefore be predicted to be 4.00×10^{19} nvt (>1 MeV).

Tensile tests were conducted at 88, 300, and 550 F on base and weld metal. In general, the yield strength and ultimate tensile strength of these metals increased due to irradiation, and the corresponding ductilities (reduction in area and total elongation) decreased.

The Charpy impact behavior was determined for base, weld, and HAZ metal. The lowest upper shelf observed was for the weld metal, which decreased from 65 to 42 ft-lb due to irradiation. The highest 30 ft-lb irradiated transition temperature observed was the 165 F value for the weld metal.

REFERENCES

- (1) Reuther, T. C., and Zwilsky, K. M., "The Effects of Neutron Irradiation on the Toughness and Ductility of Steels", in Proceedings of Toward Improved Ductility and Toughness Symposium, published by Iron and Steel Institute of Japan (October, 1971), pp 289-319.
- (2) Steele, L. E., "Major Factors Affecting Neutron Irradiation Embrittlement of Pressure-Vessel Steels and Weldments", NRL Report 7176 (October 30, 1970).
- (3) Berggren, R. G., "Critical Factors in the Interpretation of Radiation Effects on the Mechanical Properties of Structural Metals", Welding Research Council Bulletin, 87, 1 (1963).
- (4) Witt, F. J., "Heavy-Section Steel Technology Program Semiannual Progress Report for Period Ending February 29, 1972", ORNL Report No. 4816 (October, 1972).
- (5) Hawthorne, J. R., "Radiation Effects Information Generated on the ASTM Reference Correlation-Monitor Steels", American Society for Testing and Materials Data Series Publication DS54 (1974).
- (6) Steele, L. E., and Serpan, C. Z., "Neutron Embrittlement of Pressure Vessel Steels - A Brief Review", Analysis of Reactor Vessel Radiation Effects Surveillance Programs, American Society for Testing and Materials Special Technical Publication 481 (1969), pp 47-102.
- (7) Integrity of Reactor Vessels for Light-Water Power Reactors, Report by the USAEC Advisory Committee on Reactor Safeguards (January, 1974).
- (8) ASTM Designation E185-66, "Surveillance Tests on Structural Materials in Nuclear Reactors", Book of ASTM Standards, Part 31 (1967), pp 638-642.
- (9) Yanichko, S. E., and Zula, G. C., "Wisconsin Michigan Power Co. and the Wisconsin Electric Power Co. Point Beach Unit No. 2 Reactor Vessel Radiation Surveillance Program", WCAP 7712 (June, 1971).
- (10) ASTM Designation E320-69T, "Radiochemical Determination of Cesium-137 in Nuclear Fuel Solutions", Book of ASTM Standards, Part 30 (1970), pp 1004-1009.
- (11) ASTM Designation E261-70, "Measuring Neutron Flux by Radioactivation Techniques", Book of ASTM Standards, Part 30 (1970), pp 762-772.
- (12) ASTM Designation E262-70, "Measuring Thermal-Neutron Flux by Radioactivation Techniques", Book of ASTM Standards, Part 30 (1970), pp 773-780.
- (13) ASTM Designation E263-70, "Measuring Fast-Neutron Flux by Radioactivation of Iron", Book of ASTM Standards, Part 30 (1970), pp 781-783.

- (14) ASTM Designation E264-70, "Measuring Fast-Neutron Flux by Radioactivation of Nickel", Book of ASTM Standards, Part 30 (1970), pp 787-791.
- (15) ASTM Designation E343-67T, "Fast-Neutron Flux by Activation of Molybdenum-99 Activity from Uranium-238 Fission", Book of ASTM Standards, Part 30 (1970), pp 1078-1084.
- (16) ASTM Designation E393-69T, "Measuring Fast-Neutron Flux for Analysis for Barium-140 Produced by Uranium-238 Fission", Book of ASTM Standards, Part 30 (1970), pp 1174-1180.
- (17) ASTM Designation E23, "Notched Bar Impact Testing of Metallic Materials", Book of ASTM Standards, Part 10 (1974), pp 167-183.
- (18) ASTM Designation A370-71, "Mechanical Testing of Steel Products", Book of ASTM Standards, Part 10 (1974), pp 1-52.
- (19) Private communication from D. Dill of Wisconsin Electric to J. S. Perrin of BCL (June 13, 1975).
- (20) Private communication from D. Dill of Wisconsin Electric to J. S. Perrin of BCL (May 14, 1975).
- (21) Private communication from D. Dill of Wisconsin Electric to J. S. Perrin of BCL (June 10, 1975).
- (22) Private communication from J. Zach of Wisconsin Electric to J. S. Perrin of BCL (December 6, 1974).
- (23) Bush, S. H., "Structural Materials for Nuclear Power Plants", ASTM Gillette Memorial Lecture (1974).
- (24) Serpan, C. Z., Jr., and Watson, H. E., "Mechanical Property and Neutron Spectral Analyses of the Big Rock Point Reactor Pressure Vessel", Nucl. Eng. Design, 11, 393-415 (1970).
- (25) Serpan, C. Z., Jr., and Hawthorne, J. R., "Yankee Reactor Pressure-Vessel Surveillance: Notch Ductility Performance of Vessel Steel and Maximum Service Fluence Determined from Exposure During Cores II, III, and IV", NRL Report 6616 (September 29, 1967).
- (26) Brandt, F. A., "Humboldt Bay Power Plant Unit No. 3 Reactor Vessel Steel Surveillance Program", GEGR-5492 (May, 1967).
- (27) "Analysis of First Surveillance Material Capsule from San Onofre Unit I", Southern California Edison Company (July, 1971).
- (28) Perrin, J. S., Sheckherd, J. W., and Scotti, V. G., "Examination and Evaluation of Capsule F for the Connecticut Yankee Reactor Pressure-Vessel Surveillance Program", Final Report to Connecticut Yankee Atomic Power Company (March 30, 1972).

- (29) Perrin, J. S., Sheckherd, J. W., Farmelo, D. R., and Lowry, L. M., "Point Beach Nuclear Plant Unit No. 1 Pressure Vessel Surveillance Program: Evaluation of Capsule V", Final Report to Wisconsin Electric Power Company (June 15, 1973).
- (30) Ireland, D. R., and Norris, E. B., "Influence of Neutron Irradiation on the Properties of Steels and Weld Typical of theERR Pressure Vessel After Two Power Years Operation", SWRI-1228-P-9-15 (March, 1968).
- (31) Sterne, R. H., Jr., and Steele, L. E., "Steels for Commercial Nuclear Power Reactor Pressure Vessels", Nucl. Eng. Design, 10, 259-307 (1969).

APPENDIX A

PRESSURE VESSEL MATERIAL

APPENDIX A

POINT BEACH UNIT NO. 2 PRESSURE VESSEL MATERIAL ^(a)

For the Reactor Vessel Surveillance Program, Combustion Engineering, Inc., supplied Westinghouse sections of A508 Class 2 forgings used in the core region of the Point Beach Unit No. 2 reactor pressure vessel. The sections of material were removed from the 6-1/2 inch-thick intermediate and lower shell rings (forgings No. 123V500VA1 and 122W195VA1, respectively) of the pressure vessel. In addition, a weldment made from sections of the two forgings, using weld wire representative of that used in the original fabrication, was also supplied by Combustion Engineering Inc. The forgings were produced by the Bethlehem Steel Corp. The chemical analysis and heat treatment history of the vessel material follows:

A.1 Chemical Analyses (Percent)

<u>Element</u>	<u>Forging 123V500VA1</u>	<u>Forging 122W195VA1</u>	<u>Weld Metal</u>
C	0.20	0.22	0.079
Mn	0.65	0.59	1.40
P	0.009	0.010	0.014
S	0.009	0.008	0.013
Si	0.24	0.23	0.55
Mo	0.59	0.60	0.39
Ni	0.71	0.70	0.59
Cr	0.35	0.33	0.07
V	0.010	0.010	<0.002
Cu	0.088	0.051	0.25
Co	0.004	0.010	0.013
Al	<0.005	<0.005	<0.005
N ₂	0.004	0.002	0.010

(a) This Appendix is from Yanichka, S. E., and Zula, G. C., "Wisconsin Michigan Power Co and the Wisconsin Electric Power Co. Point Beach Unit No. 2 Reactor Vessel Radiation Surveillance Program", WCAP 7712 (June, 1971).

A.2 Heat Treatment

Intermediate Shell	Heated at 1550 F for 9 1/2 hours, water quenched
Heat 123V500VA1	Tempered at 1200 F for 12 hours, air cooled
	Stress-relieved at 1125 F for 12 hours, furnace cooled
Lower Shell	Heated at 1550 F for 8 hours, water quenched
Heat 122W195VA1	Tempered at 1200 F for 12 hours, air cooled
	Stress-relieved at 1125 F for 12 hours, furnace cooled
Weldment	Stress-relieved at 1125 F for 11-1/2 hours, furnace cooled.

A.3 Machining

Test material from each shell forging was heat-treated with the shells. All test specimens were machined from the 1/4 thickness location of the forgings after performing a simulated postweld stress-relieving treatment on the test material. The test specimens represent material taken at least one forging thickness (6-1/2 inches) from the quenched ends of the forging. Specimens were machined from weld and heat-affected zone metal from a stress-relieved weldment which joined sections of the two shell ring forgings. All heat-affected zone specimens were obtained from the weld heat-affected zone of forging 122W195VA1.

Charpy V-Notch Impact Specimens

The axis of the notch of the Charpy V-notch impact specimens was machined perpendicular to the major surfaces of the shell ring forging. The longitudinal axis of the specimen was parallel to the hoop direction of the shell ring forging.

Tensile Specimens

All Tensile specimens were machined with the longitudinal axis of the specimen parallel to the hoop direction of the shell ring forging.

Wedge Opening Loading Specimens

All WOL test specimens were machined with the simulated crack in the specimen perpendicular to the hoop direction and the major surfaces of the shell ring forging. The specimens were fatigue precracked according to ASTM E399-70T.

APPENDIX B

ASTM CORRELATION MONITOR MATERIAL

APPENDIX B

ASTM CORRELATION MONITOR MATERIAL ^(a)

Correlation monitor material was supplied by the Oak Ridge National Laboratory from plate material used in the AEC-sponsored Heavy Section Steel Technology (HSST) Program. This material was obtained from a 12-inch-thick A533 Grade B, Class 1 plate (HSST Plate 02) which was provided to Subcommittee II of ASTM Committee E 10 on Radioisotopes and Radiation Effects to serve as correlation monitor material in reactor vessel surveillance programs. The plate was produced by the Lukens Steel Co. and heat treated by Combustion Engineering, Inc. The following is a tabulation of the heat treatment history and plate chemistry:

Heat Treatment History

1675 \pm 25 F - 4 hours - Air-cooled
1600 \pm 25 F - 4 hours - Water-quenched
1225 \pm 25 F - 4 hours - Furnace-cooled
1150 \pm 25 F - 40 hours - Furnace-cooled to 600 F

Plate Chemistry

	<u>C</u>	<u>Mn</u>	<u>P</u>	<u>S</u>	<u>Si</u>	<u>Ni</u>	<u>Mo</u>	<u>Cu</u>
Ladle	0.22	1.45	0.011	0.019	0.22	0.62	0.53	--
Check	0.22	1.48	0.012	0.018	0.25	0.68	0.52	0.14

(a) This appendix is from Yanichko, S. E., and Zula, G. C., "Wisconsin Michigan Power Co. and the Wisconsin Electric Power Co. Point Beach Unit No. 2 Reactor Vessel Radiation Surveillance Program", WCAP 7712 (June, 1971).

APPENDIX C

DOSIMETER COUNTING DATA

POSITRONY SAMPLE DATA SHEET

WEP

Co-60 } 1.33 MeV x 60

Co-60 x 700.00 - 4.51%

Detector: NaI Specimen Type: Co

Gamma Peak

Efficiency

Counter M.I.

31.11.58 x 60.00

Co-60 x 700.00 - 4.51%

Run No.	Sample No.	Date	Counting Position	Total Counts	Background Counts	Net Counts	Time, min	Counts/min	Sum Wt, mg	Sum vol, cc	Average density, g/cc
x	69 60.0	4-1-75	10.0 cm	320,145	75,760	244,385	4.0	61,096	6.9	0.554	1.700
-	70 60.0	4-1-75	10.0 cm	123,853	63,660	60,193	4.0	15,048	11.0	0.554	1.700
-	71 60.0	4-1-75	10.0 cm	113,584	59,311	54,273	4.0	13,568	11.0	0.554	1.700
x	72 60.0	4-1-75	10.0 cm	211,324	47,328	163,996	4.0	40,999	11.0	0.554	1.700
-	73 60.0	4-1-75	10.0 cm	128,540	24,360	104,180	4.0	26,045	11.0	0.554	1.700
-	74 60.0	4-1-75	10.0 cm	155,423	43,560	111,863	4.0	27,966	11.0	0.554	1.700
x	75 60.0	4-1-75	10.0 cm	181,433	34,240	147,193	4.0	36,798	11.0	0.554	1.700
-	76 60.0	4-1-75	10.0 cm	127,434	20,550	106,884	4.0	26,721	11.0	0.554	1.700
-	77 60.0	4-1-75	10.0 cm	651,714	39,237	612,477	4.0	153,119	11.0	0.554	1.700
x	78 60.0	4-1-75	10.0 cm	272,813	42,460	230,353	4.0	57,588	11.0	0.554	1.700
-	79 60.0	4-1-75	10.0 cm	124,189	24,431	99,758	4.0	24,939	11.0	0.554	1.700
-	80 60.0	4-1-75	10.0 cm	167,846	47,313	120,533	4.0	30,133	11.0	0.554	1.700
x	81 60.0	4-1-75	10.0 cm	315,720	64,636	251,084	4.0	62,771	11.0	0.554	1.700
-	82 60.0	4-1-75	10.0 cm	12,851	18,491	73,566	4.0	18,392	11.0	0.554	1.700
-	83 60.0	4-1-75	10.0 cm	100,140	40,580	59,560	4.0	14,890	11.0	0.554	1.700

WEP
5/1/76

NES Cs-137 STD 4-1-75 22,272 net/min

22

195 1200

Gamma Peak 34 MeV Efficiency 92.5% Counter 21

✓ My friend
5/23/75

NES Cs-137 STD

ALL INFORMATION CONTAINED HEREIN IS UNCLASSIFIED

000000	000000	000000	001153	015331	013303	015271	012301	007252	004224
000001	004465	000001	000000	010000	011003	010000	011000	007014	003000
000002	004224	007252	007636	007622	010000	041700	000000	000000	000000
000003	004737	004735	004733	004853	004645	004633	004213	000000	000000
000004	004455	004225	004077	003713	003735	003434	003725	000000	000000
000005	003220	003224	003130	003154	003135	003002	003027	002443	002241
000006	002947	002946	002931	002923	002927	002772	002745	002604	002513
000007	002390	002275	002311	002360	002263	002246	002273	002246	002232
000008	002169	002222	002312	002357	002430	002306	002304	002224	002245
000009	002257	002237	002246	002175	002201	002152	001273	000000	000000
000010	007957	002606	002153	002223	002153	002134	002131	002020	002117
000011	002184	002045	001273	001553	001402	001310	001254	001140	001406
000012	001257	001259	001551	002953	001411	000433	000435	000773	000728
000013	004533	001515	000532	000532	000560	000555	000574	001031	000000
000014	000530	000603	001272	003612	000744	000435	000467	000461	000466
000015	004738	013232	005522	000424	000339	000241	000322	000321	000366
000016	000326	000322	000315	000324	000331	000340	000343	000342	000242
000017	000317	000307	000302	000374	000327	000325	000360	000313	000236
000018	000320	000246	000243	000242	000240	000246	000227	000234	000234
000019	000237	000234	000207	000215	000201	000201	000145	000201	000140

$\frac{2.470 \text{ eV}}{C^{137}}$.66 MeV

(2)

$2.01 \times 10^5 \mu\text{m}$
4/21/75

$$RKG = \frac{728 + 539}{2} \times 7 = 4435$$

Gross 120m =	10,170
B & B 120m =	4435
Net 120m =	<u>5735</u>
B & B 120m =	287

$$\begin{array}{r} 137322 \\ 276 \end{array}$$

$C_{1/2} = 4.5$

$$\begin{array}{r} 7.5 \times 10^3 \\ \times 1.2 \\ \hline 9.0 \times 10^3 \end{array}$$

6/27/75 GELI CI F.P. #2 VP 237 TXL LIG. PLASTIC ^{VIAL} "A" 10.0 giv
 AT XCEL TOP 1000V 8X2206 14RVFS 200CH 5 KEVCH 1500 HRS

001000 000002 000007 002003 041301 034943 030026 027335 025126 020425
 022245 026336 026332 032797 044554 039371 032554 034056 119913 123320
 025206 043844 033268 014793 012950 018934 051036 014313 020419 015370
 014306 013377 012932 011935 010073 009443 008749 008351 007320 004016
 007009 007191 006642 005831 005711 005595 005610 005191 005007 004343
 004334 004677 004538 005170 004299 004315 003967 004214 010305 015132
 012333 036303 007256 002796 002310 002319 006674 003323 002527 002552
 002437 002480 002452 003034 003206 002503 002533 002619 004644 002471
 002461 003845 004313 002462 002909 002503 002509 002462 002499 002507
 002620 002768 002692 002624 002624 002514 002497 002745 003333 002622
 003122 004125 002731 002607 02747 002719 002643 002664 002639 002699
 002347 002811 002551 002315 001934 001655 001432 001377 001432 001431
 001367 001171 0011203 001579 001004 000833 000942 000350 000749 000723
 001352 006159 001536 000496 000511 000433 000449 000559 000963 000522
 000417 000409 000597 002776 004104 000631 000351 000359 000362 001041
 005510 006647 019312 006165 000212 000156 000152 000160 000135 000177
 000158 000144 000142 000155 000161 000140 000153 000147 000123 000133
 000129 000123 000126 000126 000141 000133 000135 000149 000132 000126
 000123 000124 000120 000116 000097 000093 000093 000121 000124 000124
 000113 000105 000100 000093 000107 000100 000105 000115 000103 000100

Co 137

Avg Value

A 761.8

B 748.7

Avg 755.2

$$0.01585 \frac{c}{d} \text{ See Gamma Ray Spec Log Book 1/8/69}$$

$$= 4.765 \times 10^4 \text{ dpm}$$

$$= 794 \text{ dps} / 20 \text{ mg Na}_2\text{O}_2$$

$$A = 39.7 \text{ dps/mg} \times 50 \text{ DF}$$

$$= 1.985 \times 10^3 \text{ dps/mg}$$

$$\text{BKG} = \frac{723 + 496}{2} \times 5 = 304.5$$

$$\text{Gross } \%/\text{M} = 10,816$$

$$\text{BKG } \%/\text{M} = 304.5$$

$$\text{NET } \%/\text{M} = 776.8$$

$$\text{NET } \%/\text{M} = 776.8$$

$$- \text{Co 137 BKG} = 15$$

$$\text{TOTAL NET } \%/\text{M} = 761.8$$

APPENDIX D

DOSIMETER AND CAPSULE EXAMINATION



Westinghouse Electric Corporation. Power Systems

Nuclear Service Division

Box 355
Pittsburgh Pennsylvania 15230

May 1, 1975

WES 75-44

✓ Mr. T. J. Rodgers
Wisconsin Electric Power Company
231 West Michigan Street
Milwaukee, Wisconsin 53201

ATTENTION: D. L. DILL

Dear Mr. Rodgers:

SUBJECT: POINT BEACH UNITS #1 & #2 REACTOR VESSEL SURVEILLANCE
CAPSULE INFORMATION

Reference: PBM-WMP-1572 (April 8, 1975)

We believe the attached information will answer your questions as outlined in the above reference. Westinghouse will consider the subjects of new heatup and cooldown curves and reactor vessel compliance to 10CFR50 Appendix G for the Point Beach Units as pending action unless otherwise directed.

If you have any questions on either of these matters, please contact me.

Sincerely,

James S. Taylor
J. S. Taylor, Project Engineer
Operating Plants Service

JST/fak
Attachment

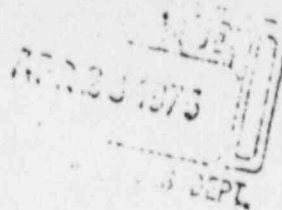
cc: G. A. Reed
J. D. Trotter
S. E. Yanichko
R. S. Longdon/WEP 1.2
File: WEP 1060



WRD - PWRSD Engineering
Mechanics and Materials Technology
236-4802

From
WIN
Date
Subject

April 21, 1975
Point Beach Unit No. 1 and 2
Reactor Vessel Surveillance Capsules



Ref: Wisconsin Electric Power Co. Letter PBM-WMP-1572, April 8, 1975

to J. S. Taylor
Field Operations, North Region
NSD

cc: J. N. Chirigos
J. A. Davidson
J. H. Phillips
T. M. Anderson
→ R. S. Longdon

The following information regarding dosimeters and capsule lead factors for the Point Beach Unit No. 1 and 2 reactor vessel surveillance capsules has been prepared in response to the Wisconsin Electric Power Company referenced letter.

1. U-238 and Np-237 Dosimeters

Dosimeter Block No.	Unit No. 1				Capsule Identification Letter ^{DID} (WCAP-7513)
	U ₃ O ₈ mg	U ²³⁸ Purity %	NpO ₂ mg	Np ²³⁷ Purity %	
35	11.52	99.9	20	99.9	V
36	9.68	99.9	20	99.9	R
37	13.21	99.9	20	99.9	T
38	8.82	99.9	20	99.9	S
39	11.26	99.9	20	99.9	N
40	9.90	99.9	20	99.9	P
	Unit No. 2				(WCAP-7712)
	U ₃ O ₈ mg	U ²³⁸ Purity %	NpO ₂ mg	Np ²³⁷ Purity %	
68	10.96	99.9	20	99.9	V
69	11.91	99.9	20	99.9	R
70	10.28	99.9	20	99.9	S
71	12.00	99.9	20	99.9	T
72	12.00	99.9	20	99.9	N
73	12.00	99.9	20	99.9	P

The weight of NpO₂ and U₃O₈ was measured to an accuracy of $\pm 0.2\%$. The neptunium oxide was ordered with a U²³⁵ and U²³⁸ content of less than 300 ppm and a Pu ²³⁹ content of less than 500 ppm. The uranium oxide was ordered with a U²³⁵ content of less than 300 ppm.

April 21, 1975

2. Copper Dosimeters

- a. The weight of the copper dosimeters was not determined.
- b. The purity of the copper dosimeters was reported as 99.999% by the supplier.
- c. A chemical analysis performed by the supplier resulted in the detection on no impurities.

3. Capsule Lead Factors for Units No. 1 and 2

<u>Capsule Identification</u>	<u>Capsule Position (degrees)</u>	<u>Lead Factors</u>
V	77	2.5
R	257	2.5
T	67	1.6
P	247	1.6
S	57	1.4
N	237	1.4

*S. E. Yanichko*S. E. Yanichko
Structural Materials Engineering

/lat

APPENDIX E

INSTRUMENTED CHARPY EXAMINATION

APPENDIX E

INSTRUMENTED CHARPY EXAMINATION

SUMMARY

The instrumented Charpy technique was applied to the impact specimen evaluations of the following pressure vessel materials: base metal, weld metal, heat-affected-zone metal, and ASTM correlation monitor metal. Because of the limited number of specimens and their need in establishing other parameters such as the upper shelf energy and the ductile-brittle transition temperature, there were insufficient data available for a complete analysis on these materials. However, load-time traces were obtained which show the change in impact behavior as a function of temperature for each of the materials tested.

INTRODUCTION

The radiation embrittlement of an operating nuclear pressure vessel is determined by the accelerated irradiation of the original materials as part of a surveillance program. The lifetime of the pressure vessel will depend on the radiation-induced shift in the ductile-brittle transition temperature as measured by the Charpy V-notch impact test.

The value of Charpy impact specimens, particularly in present surveillance programs, can be considerably enhanced by the use of the instrumented Charpy test. The instrumented Charpy test provides a valuable link between the transition-temperature approach and the fracture-mechanics approach to fracture toughness. A knowledge of the effect of radiation on key metallurgical fracture parameters can be used to accurately predict (1) the radiation-induced shift in the ductile-brittle transition temperature, and (2) the radiation-induced change in the dynamic fracture toughness, K_{Id} . The results obtained by applying these techniques to the surveillance program Charpy specimens are presented in this section of the report.

BACKGROUND

There are two approaches to determining the effect of radiation on the fracture toughness of pressure-vessel steels: (1) the shift in the ductile-brittle transition temperature, and (2) the change in the fracture toughness (either the static fracture toughness K_{Ic} or the dynamic fracture toughness K_{Id}). The modern theories of fracture define key metallurgical fracture parameters such as friction stress, grain size, grain-size dependence of the yield stress, and surface energy or plastic work of microcrack propagation. The effect of radiation on most of these metallurgical fracture parameters has been previously studied, but until recently, the results had not been directly linked with the radiation-induced change in fracture toughness. This recent work established the relationships between the key metallurgical fracture parameters and the transition temperature and $K_{Ic}^{(1)}$. *

The instrumented Charpy test is an excellent tool for determination of the effects of radiation on the key metallurgical fracture parameters. This test provides load-time information in addition to the energy absorbed. The loads involved during impact are obtained by instrumenting the Charpy striker with strain gages so that the striker or tup is essentially a load cell. The details of this technique have been reported previously. ^(2,3)

The additional information obtained from the instrumented Charpy test is the general yield load, P_{GY} (plastic yielding across the entire cross section of the Charpy specimen), the maximum load, P_{max} , the brittle fracture load, P_F , and the time to brittle fracture (see Figure E-1). Also, the area under the load-time curve corresponds to the total energy absorbed, which is the only data obtained in a normal uninstrumented Charpy test. The instrumented test, however, allows separation of the energy absorbed into (1) the energy required to initiate ductile or brittle fracture (premaximum load energy), (2) the energy required for ductile tearing (postmaximum load energy), and (3) the energy associated with shear lip formation (postbrittle fracture energy), as shown in Figure E-1.

* References at the end of this Appendix.

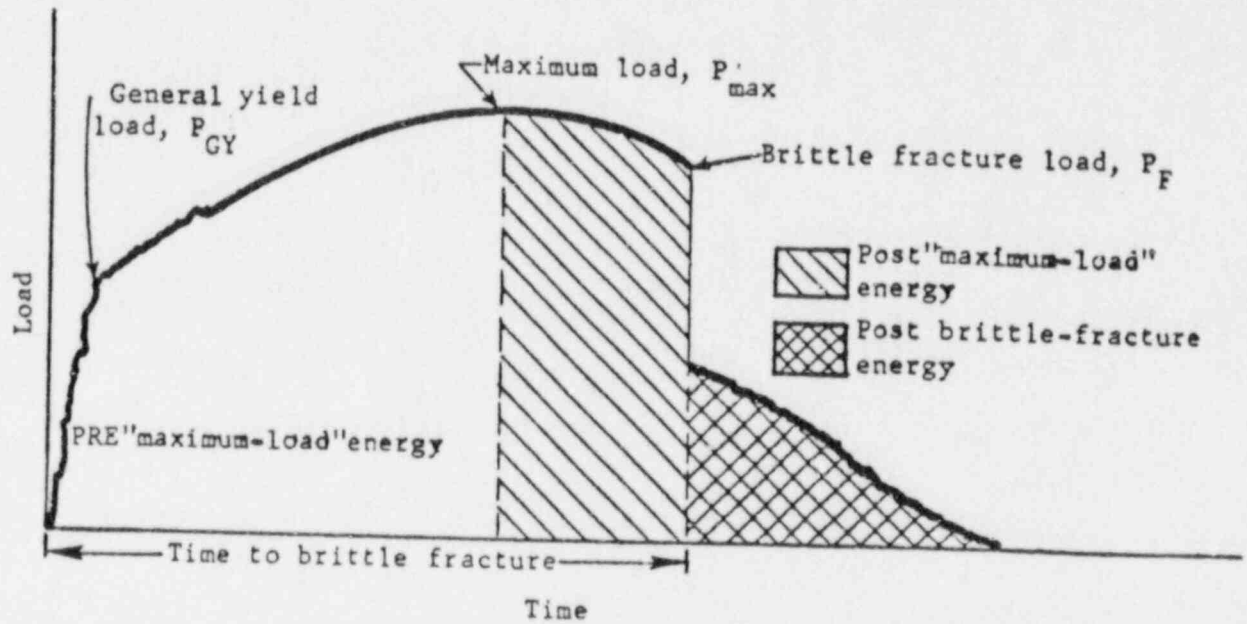


FIGURE E-1. AN IDEALIZED LOAD-TIME HISTORY FOR A CHARPY IMPACT TEST

In a normal Charpy impact study, the energy absorbed is determined as a function of temperature to obtain the Charpy impact curve and the transition temperature. The instrumented Charpy test also gives the information shown in Figure E-1 as a function of temperature, as shown by the example in Figure E-2. Various investigators⁽⁴⁻⁷⁾ have developed theories that permit a detailed analysis of the load-temperature diagram. This diagram can be divided into four regions of fracture behavior, as shown in Figure E-2. In each region different fracture parameters are involved⁽²⁾. Extended discussions of these fracture parameters can be found in the references indicated above.

In general, the key metallurgical fracture parameters for radiation damage studies are the cleavage fracture stress, σ_f^* , and the yield strength, σ_y . Both of these parameters and the temperature sensitivity of σ_y can be derived from the results of the instrumented Charpy tests. The determination of the cleavage fracture stress σ_f^* , requires an evaluation of P_{GY} at the temperature where P_F is 80 percent of P_{GY} . The yield strength, σ_y , is calculated from the general yield load, P_{GY} , and is related to the uniaxial tensile strength, σ_{YS} , by the relation⁽⁷⁾:

$$\sigma_{YS} = 33.3 P_{GY}.$$

This relation is for a standard Charpy V-notch specimen, is dependent on the flank angle of the notch, and assumes Tresca yield criterion.

EXPERIMENTAL PROCEDURES

The general procedures for the instrumented Charpy test are the same as those for the conventional impact test, and are described in the main text of this report. The additional data are obtained through a fairly simple electronic configuration, as shown in the schematic diagram of Figure E-3.

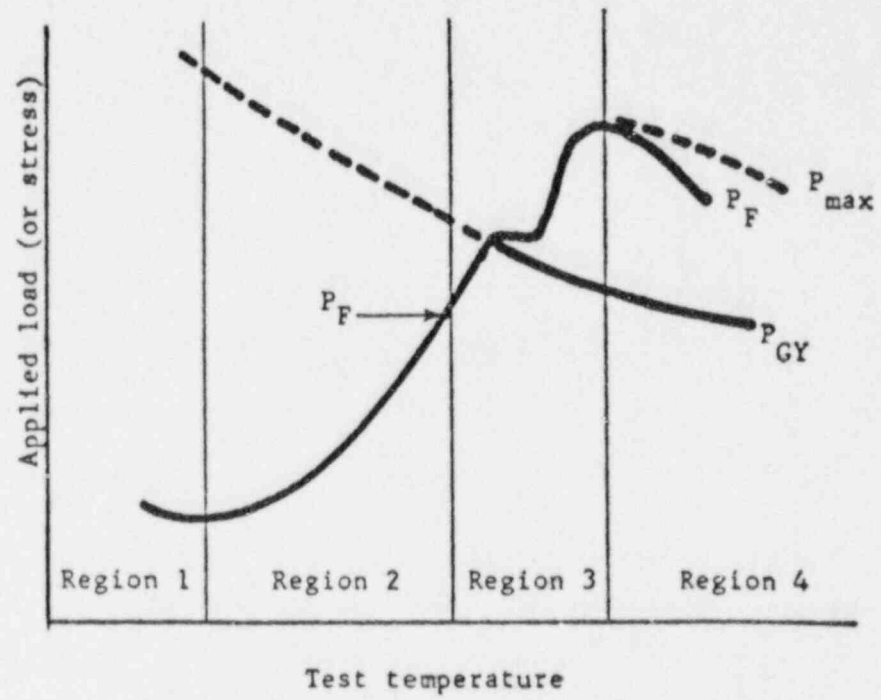


FIGURE E-2. GRAPHICAL ANALYSIS OF CHARPY IMPACT DATA

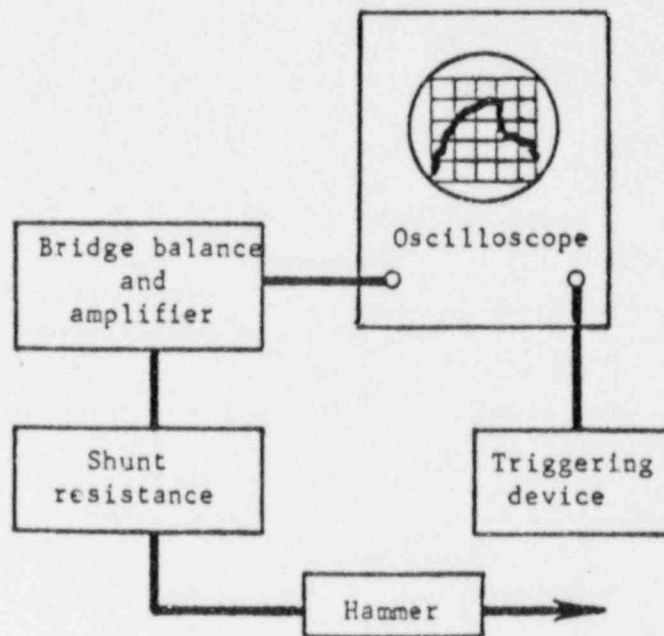


FIGURE E-3. DIAGRAM OF INSTRUMENTATION ASSOCIATED WITH INSTRUMENTED CHARPY EXAMINATION

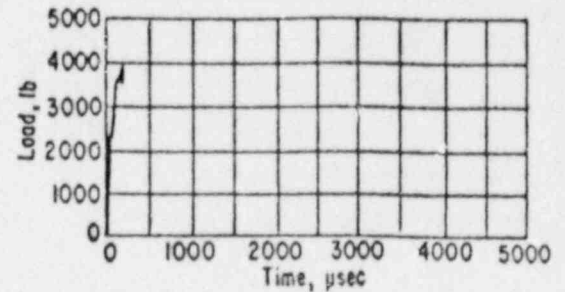
The striker of the impact machine is modified to make it a dynamic load sensor. The modification consists of a four-arm resistance strain gage bridge positioned on the striker to detect the compression loading of the striker during the impact loading of the specimen. The compressive elastic strain signal resulting from the striker contacting the specimen is conditioned by a high-gain dynamic amplifier and the output is photographed as it develops on the cathode ray tube of an oscilloscope. A previously established calibration method⁽⁹⁾ is used to convert the oscillograph into a time-load record. The time-load history as a function of test temperature forms the basis for further data analysis. The oscilloscope is triggered by a solid-state device at the correct time to capture the amplifier output signal.

RESULTS AND DISCUSSION

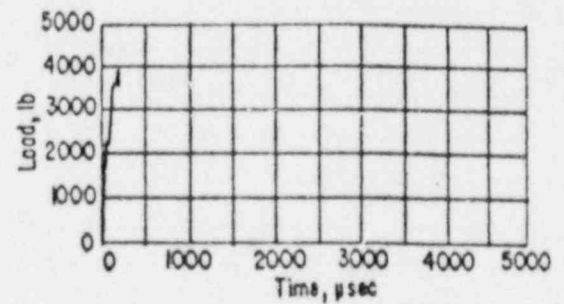
The instrumented Charpy tests were conducted following the procedures discussed in the main text of this report. Specimens were tested from four irradiated materials. These materials were the pressure vessel base metal, weld metal, heat-affected-zone metal, and ASTM correlation monitor metal. The results of the instrumented Charpy work with the corresponding load-time records are given in Tables E-1 through E-5. The tables list the specimen numbers, test temperature, impact energy, general yield load, and maximum load. Some curves are not shown because they were not obtained on the oscilloscope. It can readily be observed that the features of the load-time or load-deflection traces change as a function of temperature; however, all tests fall into one of the six distinctive notch-bar bending classifications shown in Figure E-4. The pertinent data used in the analysis of each record are the general yield load (P_{GY}), maximum load (P_{max}), and fracture load (P_F). The impact energy values listed in the tables are those normally obtained from the impact machine dial. These values are in excellent agreement with energy values from the area under the load-time curves.

TABLE E-1. INSTRUMENTED CHARPY IMPACT DATA FOR BASE-METAL
PLATE 122W195VA1 FROM POINT BEACH UNIT 2

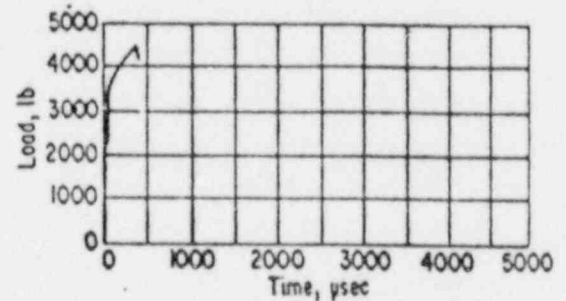
Specimen No.	E1
Test Temperature, F	-80
Impact Energy, ft-lb	8.0
General Yield Load, P_{GY} , lb	
Maximum Load, P_{max} , lb	3950



Specimen No.	E3
Test Temperature, F	-80
Impact Energy, ft-lb	7.5
General Yield Load, P_{GY} , lb	
Maximum Load, P_{max} , lb	3900



Specimen No.	E8
Test Temperature, F	-45
Impact Energy, ft-lb	25.5
General Yield Load, P_{GY} , lb	
Maximum Load, P_{max} , lb	4350



Specimen No.	E2
Test Temperature, F	0
Impact Energy, ft-lb	58.5
General Yield Load, P_{GY} , lb	3200
Maximum Load, P_{max} , lb	4400

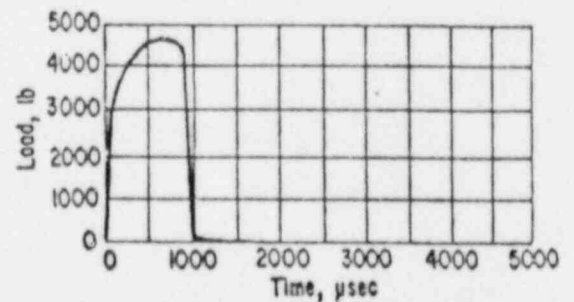
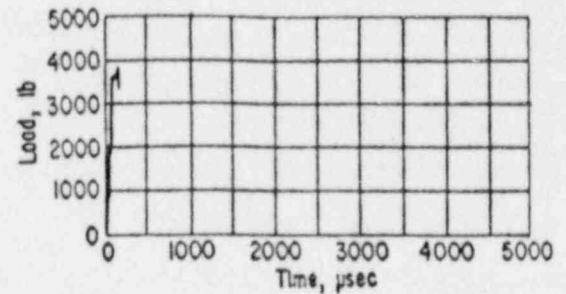
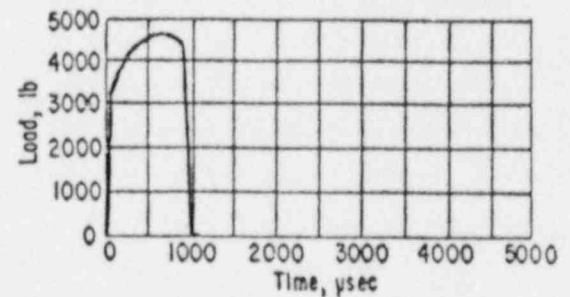


TABLE E-1 (Continued)

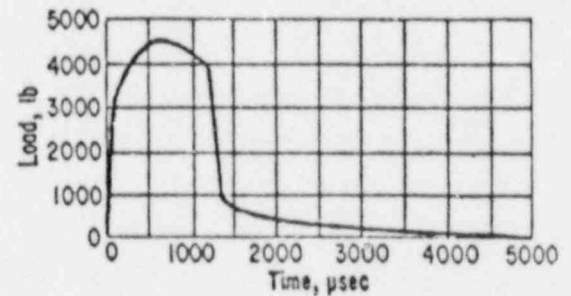
Specimen No.	E4
Test Temperature, F	0
Impact Energy, ft-lb	10.5
General Yield Load, P_{GY} , lb	
Maximum Load, P_{max} , lb	3700



Specimen No.	E9
Test Temperature, F	0
Impact Energy, ft-lb	55.0
General Yield Load, P_{GY} , lb	3300
Maximum Load, P_{max} , lb	4450



Specimen No.	E7
Test Temperature, F	74
Impact Energy, ft-lb	86.0
General Yield Load, P_{GY} , lb	3000
Maximum Load, P_{max} , lb	4250



Specimen No.	E11
Test Temperature, F	76
Impact Energy, ft-lb	76.5
General Yield Load, P_{GY} , lb	3050
Maximum Load, P_{max} , lb	4050

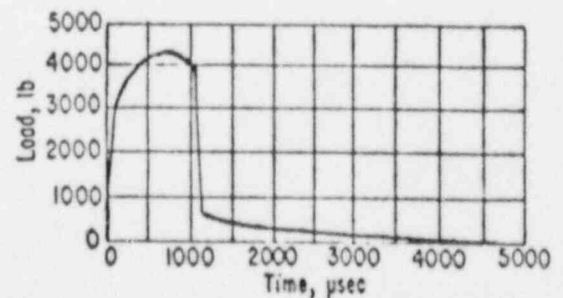
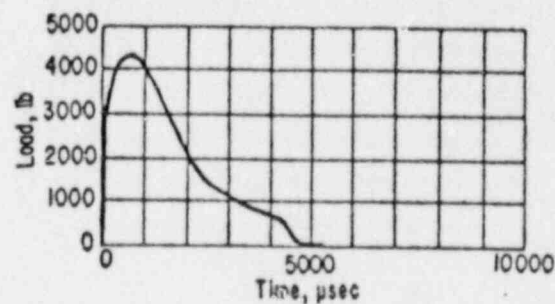
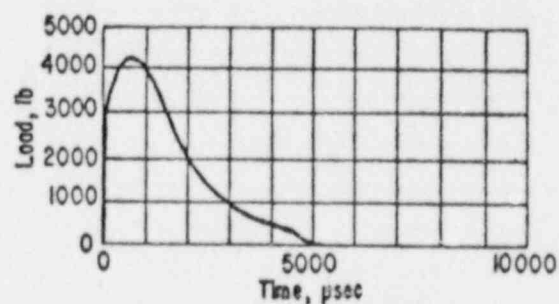


TABLE E-1 (Continued)

Specimen No.	E5
Test Temperature, F	145
Impact Energy, ft-lb	141.5
General Yield Load, P_{GY} , lb	2850
Maximum Load, P_{max} , lb	4150



Specimen No.	E6
Test Temperature, F	145
Impact Energy, ft-lb	133.0
General Yield Load, P_{GY} , lb	2950
Maximum Load, P_{max} , lb	4100



Specimen No.	E12
Test Temperature, F	200
Impact Energy, ft-lb	136.5
General Yield Load, P_{GY} , lb	
Maximum Load, P_{max} , lb	

Specimen No.	E10
Test Temperature, F	290
Impact Energy, ft-lb	135.0
General Yield Load, P_{GY} , lb	2750
Maximum Load, P_{max} , lb	3900

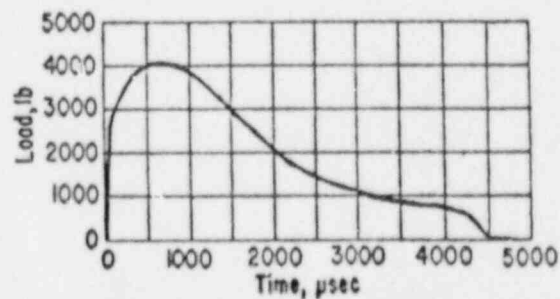
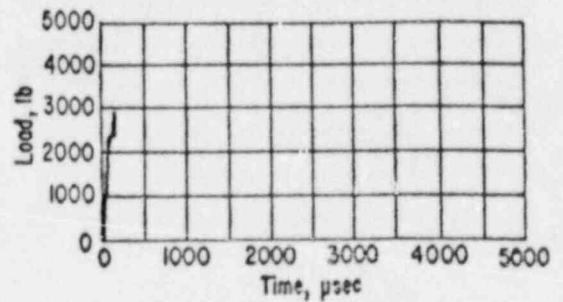
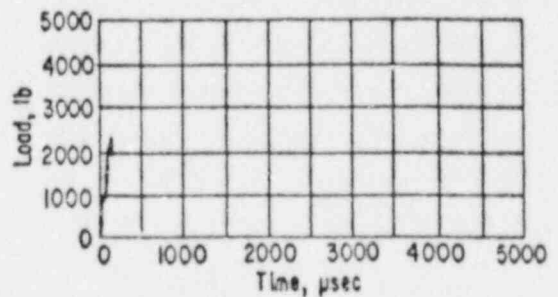


TABLE E-2. INSTRUMENTED CHARPY IMPACT DATA FOR BASE-METAL
PLATE 123V500VA1 FROM POINT BEACH UNIT 2

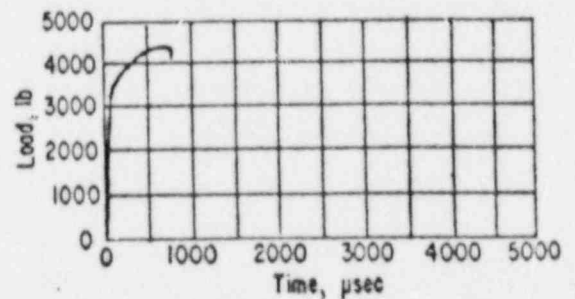
Specimen No.	V10
Test Temperature, F	-80
Impact Energy, ft-lb	3.5
General Yield Load, P_{GY} , lb	
Maximum Load, P_{max} , lb	2900



Specimen No.	V3
Test Temperature, F	-80
Impact Energy, ft-lb	2.0
General Yield Load, P_{GY} , lb	
Maximum Load, P_{max} , lb	2500



Specimen No.	V6
Test Temperature, F	-45
Impact Energy, ft-lb	50.5
General Yield Load, P_{GY} , lb	3200
Maximum Load, P_{max} , lb	4250



Specimen No.	V1
Test Temperature, F	-45
Impact Energy, ft-lb	22.0
General Yield Load, P_{GY} , lb	
Maximum Load, P_{max} , lb	4250

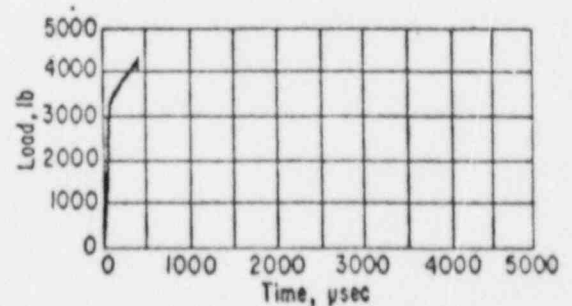
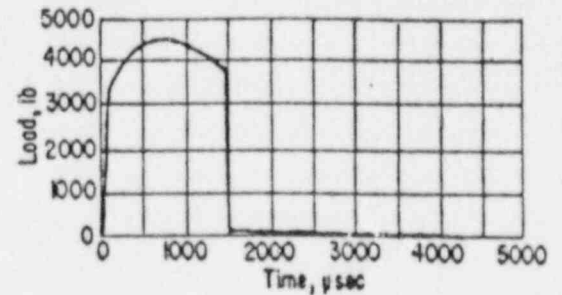


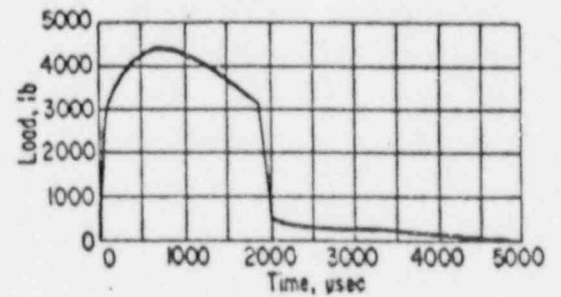
TABLE E-2 (Continued)

Specimen No.	V2
Test Temperature, F	0
Impact Energy, ft-lb	90
General Yield Load, P_{GY} , lb	
Maximum Load, P_{max} , lb	

Specimen No.	V11
Test Temperature, F	0
Impact Energy, ft-lb	94.5
General Yield Load, P_{GY} , lb	3200
Maximum Load, P_{max} , lb	4350



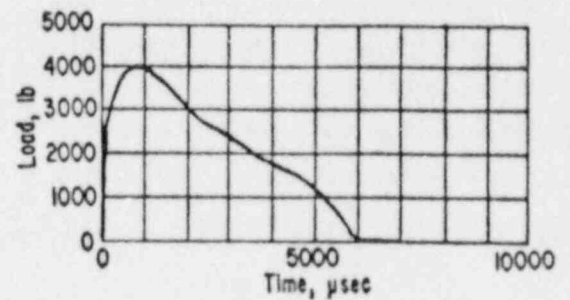
Specimen No.	V12
Test Temperature, F	74
Impact Energy, ft-lb	114.5
General Yield Load, P_{GY} , lb	2950
Maximum Load, P_{max} , lb	4250



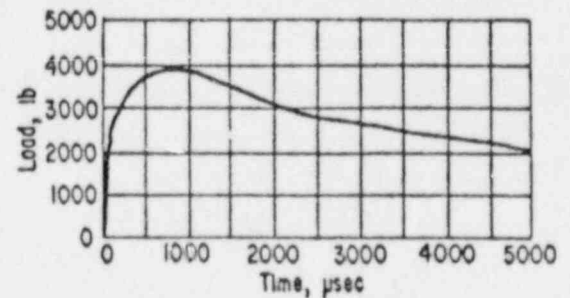
Specimen No.	V7
Test Temperature, F	76
Impact Energy, ft-lb	108.5
General Yield Load, P_{GY} , lb	
Maximum Load, P_{max} , lb	

TABLE E-2 (continued)

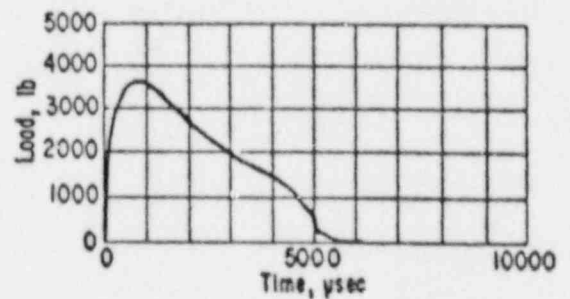
Specimen No.	V5
Test Temperature, F	145
Impact Energy, ft-lb	186.5
General Yield Load, P_{GY} , lb	2550
Maximum Load, P_{max} , lb	3800



Specimen No.	V4
Test Temperature, F	200
Impact Energy, ft-lb	216.0
General Yield Load, P_{GY} , lb	2400
Maximum Load, P_{max} , lb	3600



Specimen No.	V9
Test Temperature, F	290
Impact Energy, ft-lb	165.0
General Yield Load, P_{GY} , lb	2500
Maximum Load, P_{max} , lb	3550



Specimen No.	V8
Test Temperature, F	345
Impact Energy, ft-lb	198.5
General Yield Load, P_{GY} , lb	2300
Maximum Load, P_{max} , lb	3450

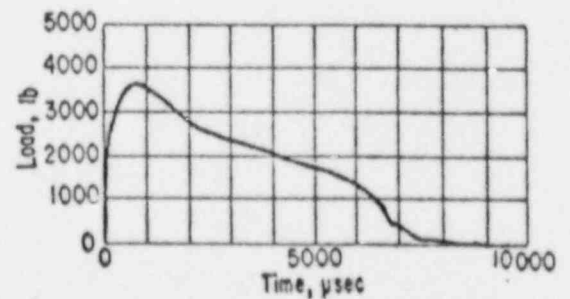
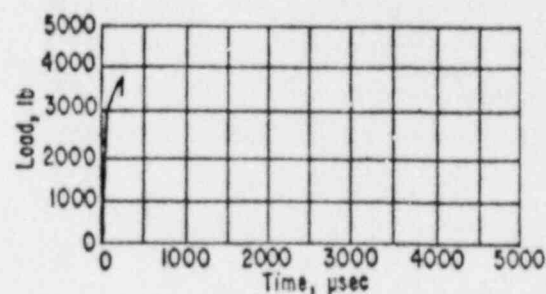
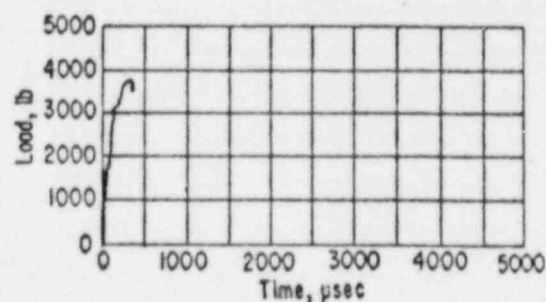


TABLE E-3. INSTRUMENTED CHARPY IMPACT DATA FOR WELD METAL FROM POINT BEACH UNIT 2

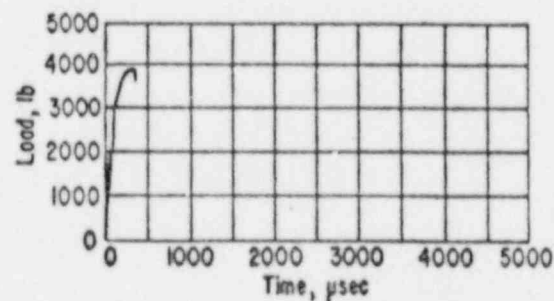
Specimen No.	W6
Test Temperature, F	76
Impact Energy, ft-lb	13.5
General Yield Load, P_{GY} , lb	
Maximum Load, P_{max} , lb	3800



Specimen No.	W3
Test Temperature, F	145
Impact Energy, ft-lb	22.5
General Yield Load, P_{GY} , lb	
Maximum Load, P_{max} , lb	3800



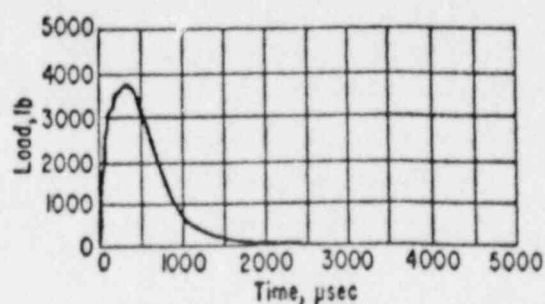
Specimen No.	W5
Test Temperature, F	145
Impact Energy, ft-lb	27.0
General Yield Load, P_{GY} , lb	
Maximum Load, P_{max} , lb	3850



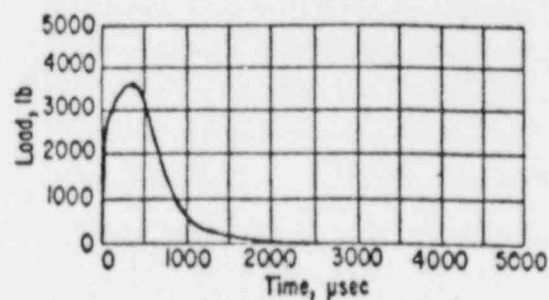
Specimen No.	W8
Test Temperature, F	200
Impact Energy, ft-lb	43.0
General Yield Load, P_{GY} , lb	
Maximum Load, P_{max} , lb	

TABLE E-3 (Continued)

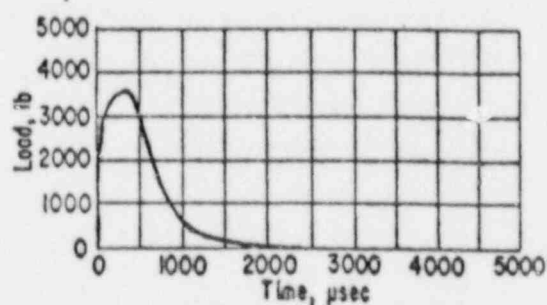
Specimen No.	W1
Test Temperature, F	290
Impact Energy, ft-lb	41.5
General Yield Load, P_{GY} , lb	3050
Maximum Load, P_{max} , lb	3550



Specimen No.	W7
Test Temperature, F	310
Impact Energy, ft-lb	41.0
General Yield Load, P_{GY} , lb	2750
Maximum Load, P_{max} , lb	3450



Specimen No.	W2
Test Temperature, F	345
Impact Energy, ft-lb	41.5
General Yield Load, P_{GY} , lb	2750
Maximum Load, P_{max} , lb	3500



Specimen No.	W4
Test Temperature, F	345
Impact Energy, ft-lb	43.5
General Yield Load, P_{GY} , lb	3000
Maximum Load, P_{max} , lb	3550

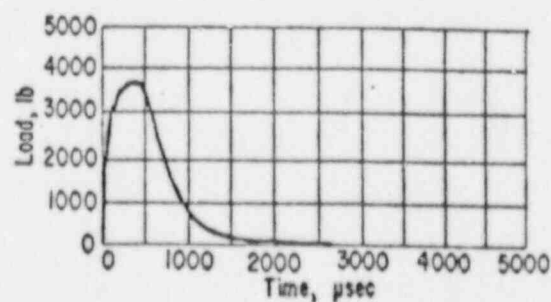
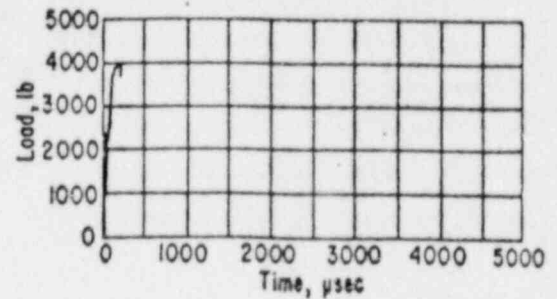
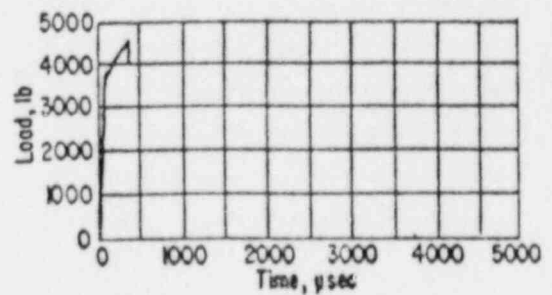


TABLE E-4. INSTRUMENTED CHARPY IMPACT DATA FOR HEAT-AFFECTED ZONE METAL FROM POINT BEACH UNIT 2

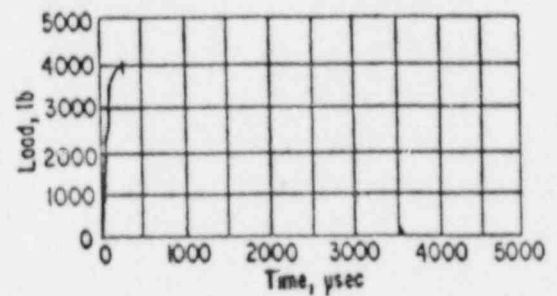
Specimen No.	H2
Test Temperature, F	0
Impact Energy, ft-lb	10.5
General Yield Load, P_{GY} , lb	
Maximum Load, P_{max} , lb	4000



Specimen No.	H5
Test Temperature, F	0
Impact Energy, ft-lb	27.0
General Yield Load, P_{GY} , lb	
Maximum Load, P_{max} , lb	4400



Specimen No.	H8
Test Temperature, F	0
Impact Energy, ft-lb	15.0
General Yield Load, P_{GY} , lb	
Maximum Load, P_{max} , lb	4100



Specimen No.	H1
Test Temperature, F	76
Impact Energy, ft-lb	115.0
General Yield Load, P_{GY} , lb	3100
Maximum Load, P_{max} , lb	4350

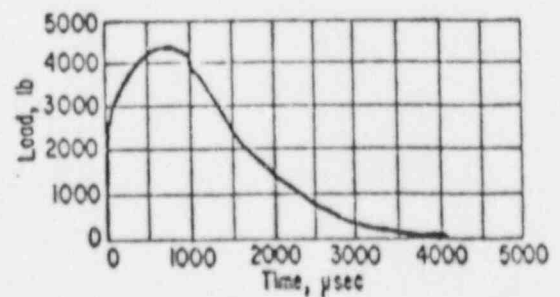
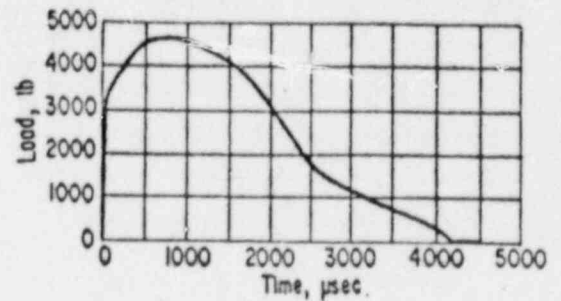
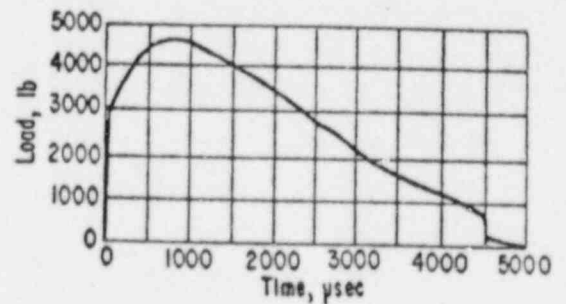


TABLE E-4 (Continued)

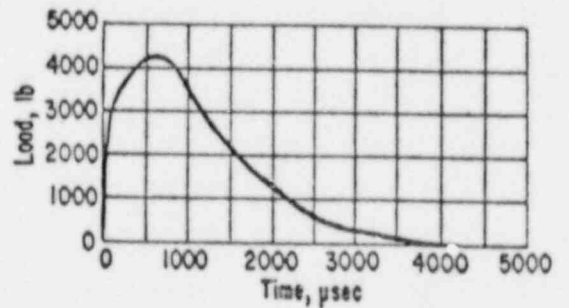
Specimen No.	H6
Test Temperature, F	76
Impact Energy, ft-lb	152.0
General Yield Load, P_{GY} , lb	3200
Maximum Load, P_{max} , lb	3450



Specimen No.	H4
Test Temperature, F	145
Impact Energy, ft-lb	177.0
General Yield Load, P_{GY} , lb	2950
Maximum Load, P_{max} , lb	3400



Specimen No.	H7
Test Temperature, F	200
Impact Energy, ft-lb	102.5
General Yield Load, P_{GY} , lb	2750
Maximum Load, P_{max} , lb	4050



Specimen No.	H3
Test Temperature, F	290
Impact Energy, ft-lb	195.0
General Yield Load, P_{GY} , lb	2800
Maximum Load, P_{max} , lb	4050

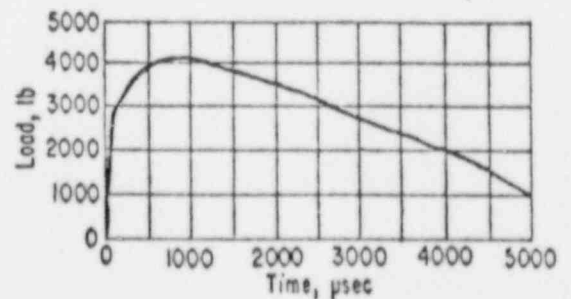
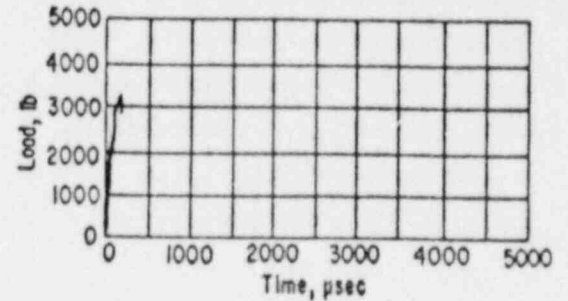
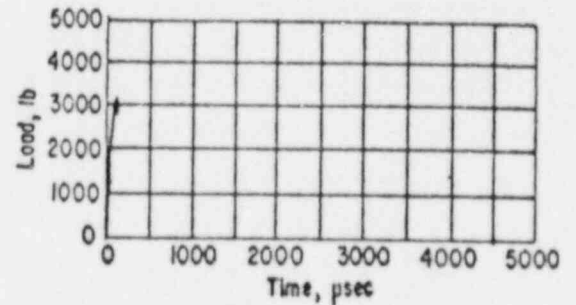


TABLE E-5. INSTRUMENTED CHARPY IMPACT DATA FOR ASTM CORRELATION
MONITOR MATERIAL FROM POINT BEACH UNIT 2

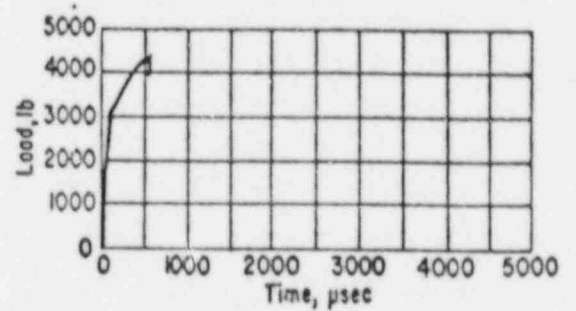
Specimen No.	R7
Test Temperature, F	76
Impact Energy, ft-lb	9.5
General Yield Load, P_{GY} , lb	
Maximum Load, P_{max} , lb	3300



Specimen No.	R2
Test Temperature, F	80
Impact Energy, ft-lb	7.0
General Yield Load, P_{GY} , lb	
Maximum Load, P_{max} , lb	3150



Specimen No.	R4
Test Temperature, F	145
Impact Energy, ft-lb	39.0
General Yield Load, P_{GY} , lb	3200
Maximum Load, P_{max} , lb	4150



Specimen No.	R5
Test Temperature, F	145
Impact Energy, ft-lb	31.0
General Yield Load, P_{GY} , lb	2950
Maximum Load, P_{max} , lb	4050

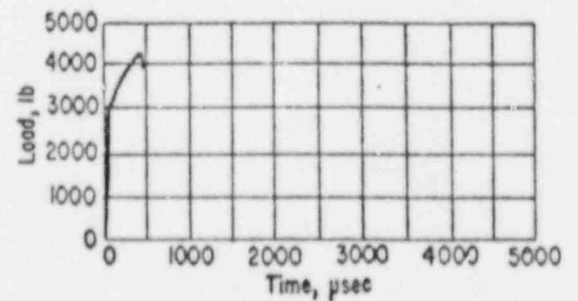
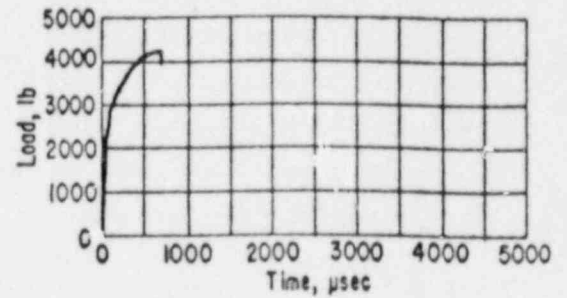


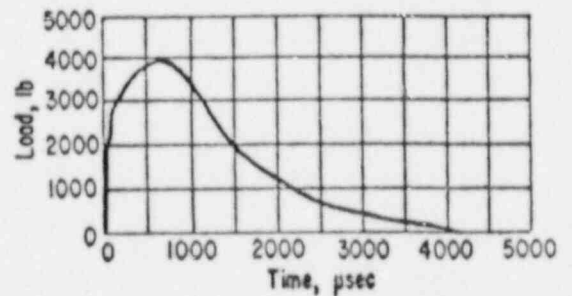
TABLE E-5 (Continued)

Specimen No.	R6
Test Temperature, F	200
Impact Energy, ft-lb	55.0
General Yield Load, P_{GY} , lb	2800
Maximum Load, P_{max} , lb	4050

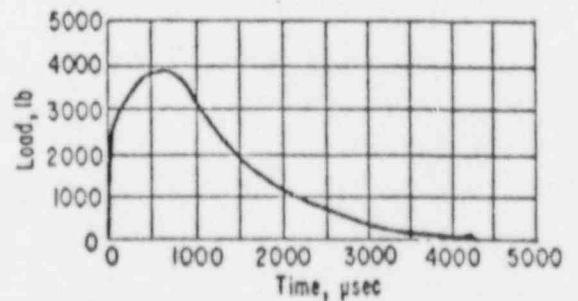


Specimen No.	R8
Test Temperature, F	290
Impact Energy, ft-lb	81.5
General Yield Load, P_{GY} , lb	
Maximum Load, P_{max} , lb	

Specimen No.	R1
Test Temperature, F	345
Impact Energy, ft-lb	96.5
General Yield Load, P_{GY} , lb	2550
Maximum Load, P_{max} , lb	3750



Specimen No.	R3
Test Temperature, F	345
Impact Energy, ft-lb	90.5
General Yield Load, P_{GY} , lb	2550
Maximum Load, P_{max} , lb	3700



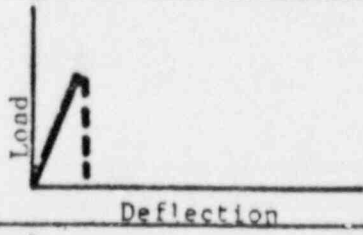
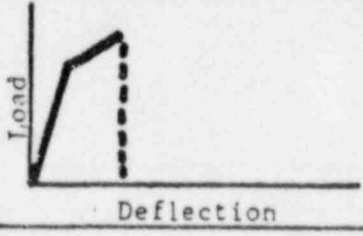
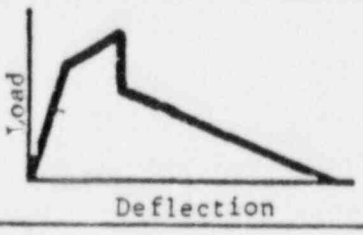
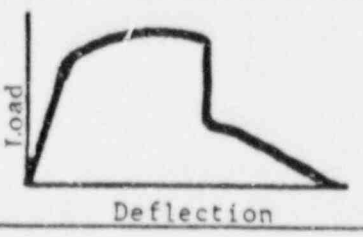
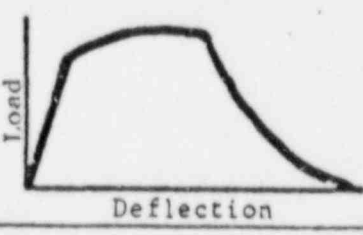
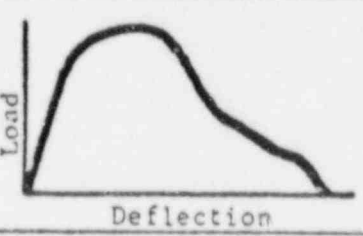
Fracture type	Load-displacement curves	Raw data	Remarks
I		P_F	Brittle fracture
II		P_{GY}	Brittle fracture
III		P_{GY}	Brittle fracture followed by fracture indicative of shear lip formation
IV		P_{GY}, P_{max}	Stable crack propagation followed by unstable brittle fracture and fracture indicative of shear lip formation
V		P_{GY}, P_{max}	Stable crack propagation followed by fracture indicative of shear lip formation
VI		P_{GY}, P_{max}	Stable crack propagation followed by gross deformation

FIGURE E-4. THE SIX TYPES OF FRACTURE FOR NOTCHED BAR BENDING

The Charpy energy curves and the load-temperature information obtained from the instrumented Charpy tests are shown in Figures E-5 through E-9. These figures illustrate a unique feature of this type of analysis; that is, the determination of a definitive fracture transition temperature by discrimination between fractures occurring below and above general yield (P_{GY}). This transition is a clear indication of the mechanical properties of the material and does not depend on empirical correlations, as the nil-ductility transition temperature (NDIT) determined by the 30 ft-lb fix temperature does. It is interesting to note that impact fracture at the 30 ft-lb level corresponds to ductile specimen behavior, where considerable work hardening is required to raise the stress at the notch to a value sufficiently above the yield stress for fracture to result. In general, the curves show both the general yield load and the maximum load initially increasing as temperature is decreased from the upper shelf region of the Charpy impact curve. As temperature is further decreased through the transition temperature region, the maximum load goes through a maximum and drops off as temperature continues to be decreased. The general yield load is also quite sensitive with respect to temperature. As the temperature is decreased from the upper shelf region, the general yield load increases substantially.

CONCLUSIONS

The instrumented Charpy impact test technique was used to study the impact behavior of pressure-vessel materials. Because of the limited number of Charpy specimens, it was not possible to do a complete analysis of these materials. However, it was shown that in all materials the nil-ductility transition temperature as determined by the 30 ft-lb fix corresponds to specimen behavior where there is some ductile behavior rather than completely brittle behavior. The maximum load was shown to go through a maximum as temperature is lowered from the upper shelf region into the transition temperature region. In addition, the general yield load was shown to increase as temperature is decreased.

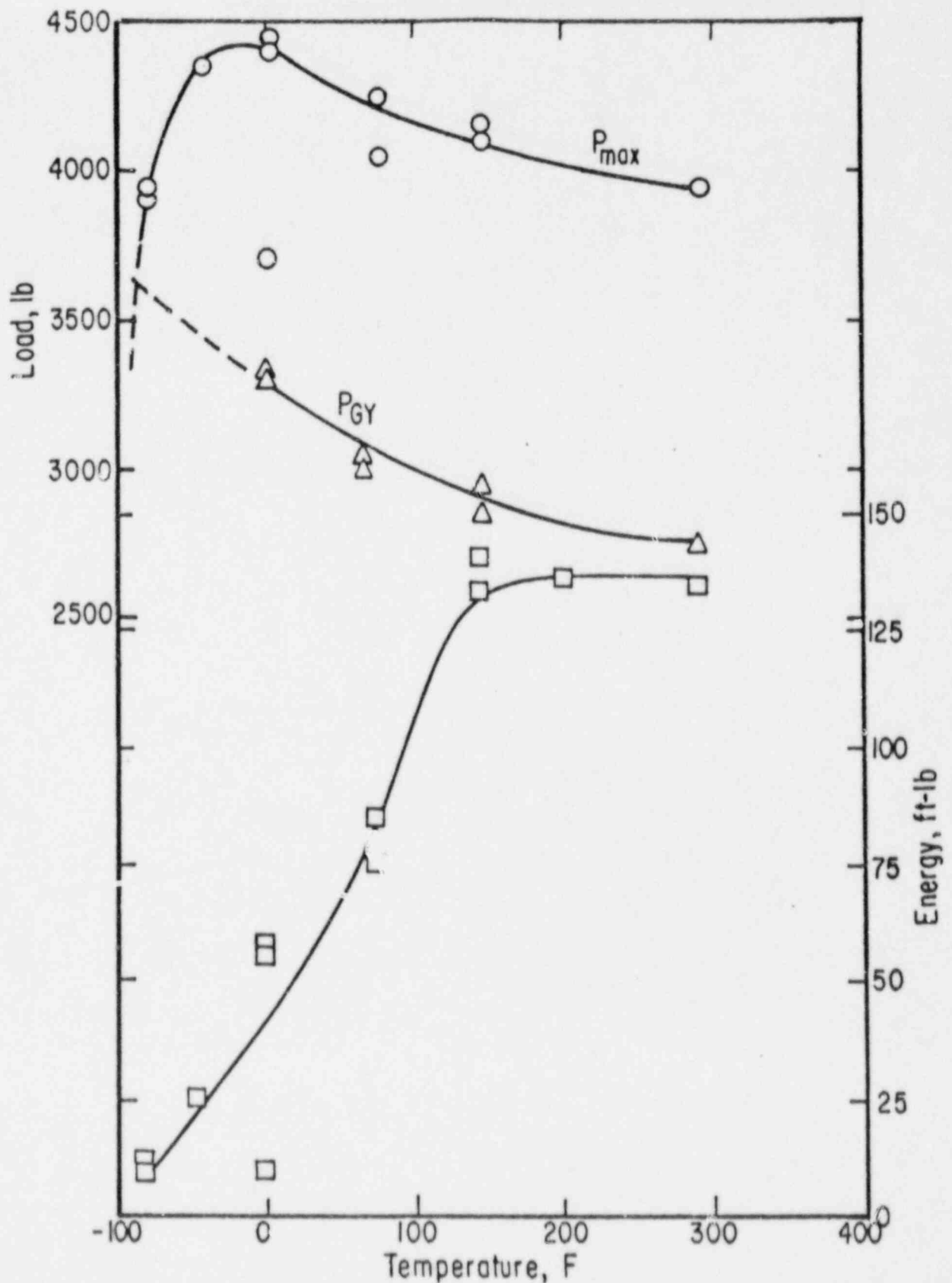


FIGURE E-5. INSTRUMENTED CHARPY LOAD-TEMPERATURE AND IMPACT ENERGY-TEMPERATURE CURVES FOR POINT BEACH UNIT NO. 2 BASE METAL PLATE 122W195VA1 (E SERIES)

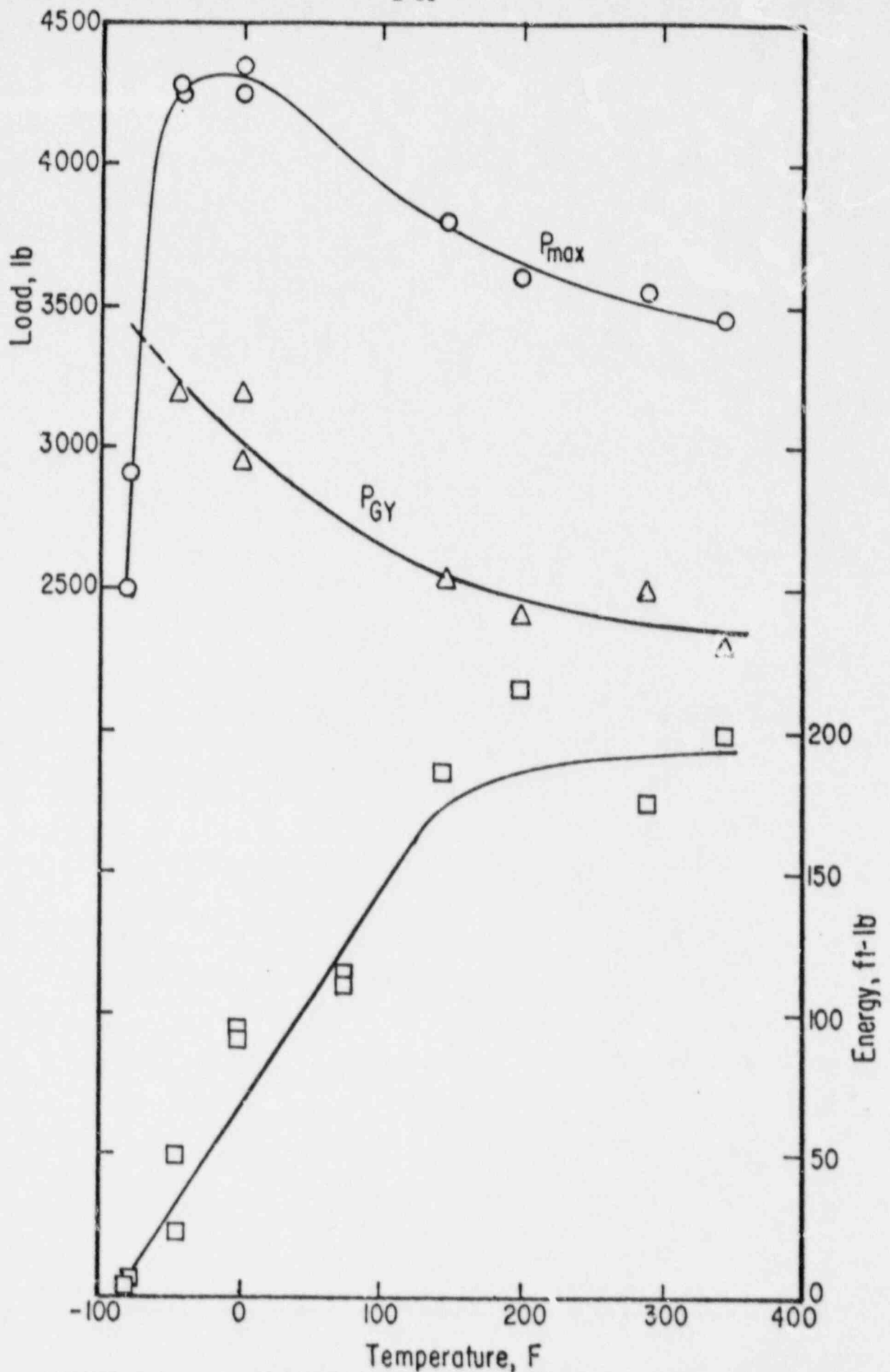


FIGURE E-6. INSTRUMENTED CHARPY LOAD-TEMPERATURE AND IMPACT ENERGY-TEMPERATURE CURVES FOR POINT BEACH UNIT NO. 2 BASE METAL PLATE 123V500VA1 (V SERIES)

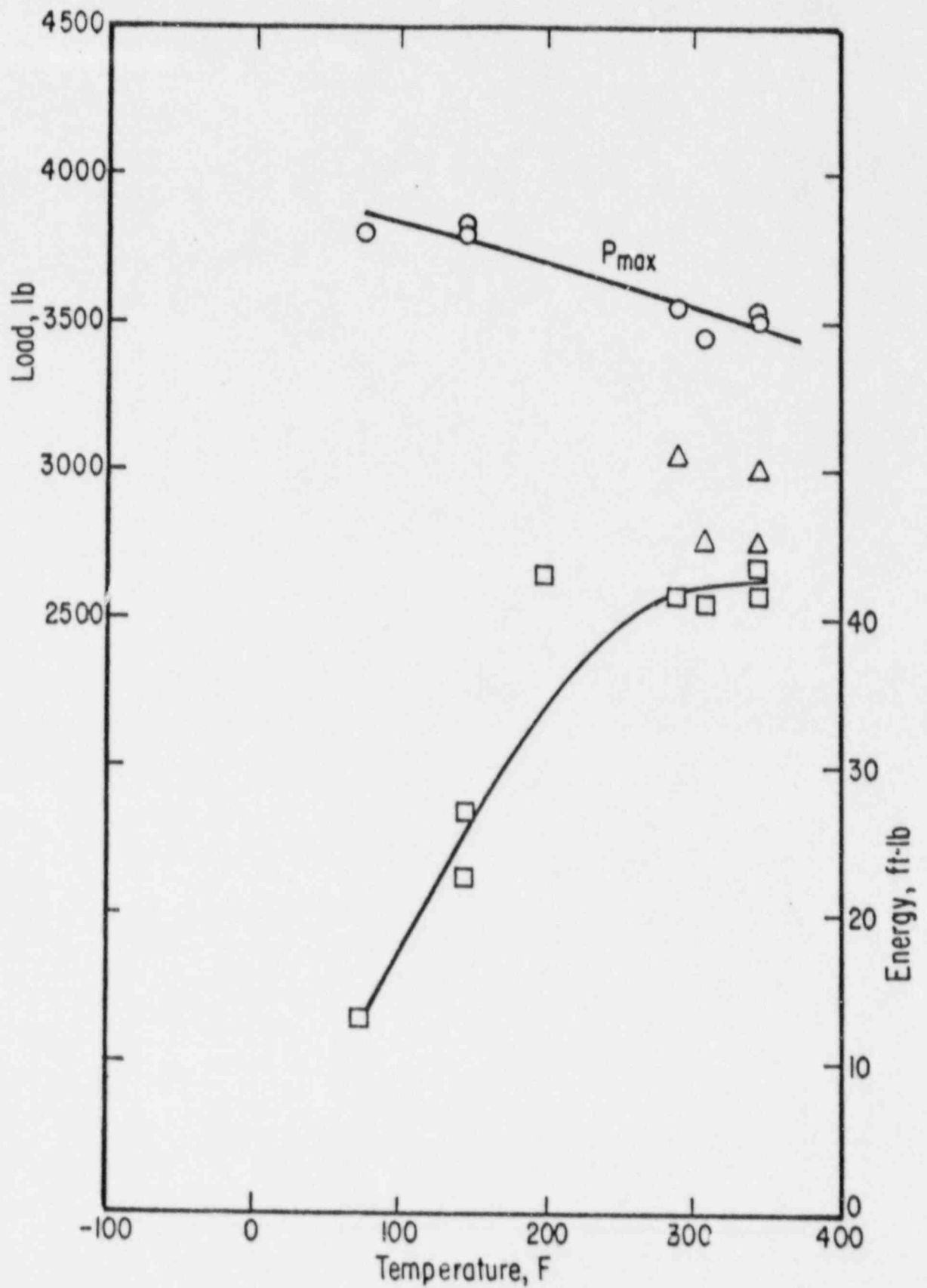


FIGURE E-7. INSTRUMENTED CHARPY LOAD-TEMPERATURE AND IMPACT ENERGY-TEMPERATURE CURVES FOR POINT BEACH UNIT NO. 2 WELD METAL.

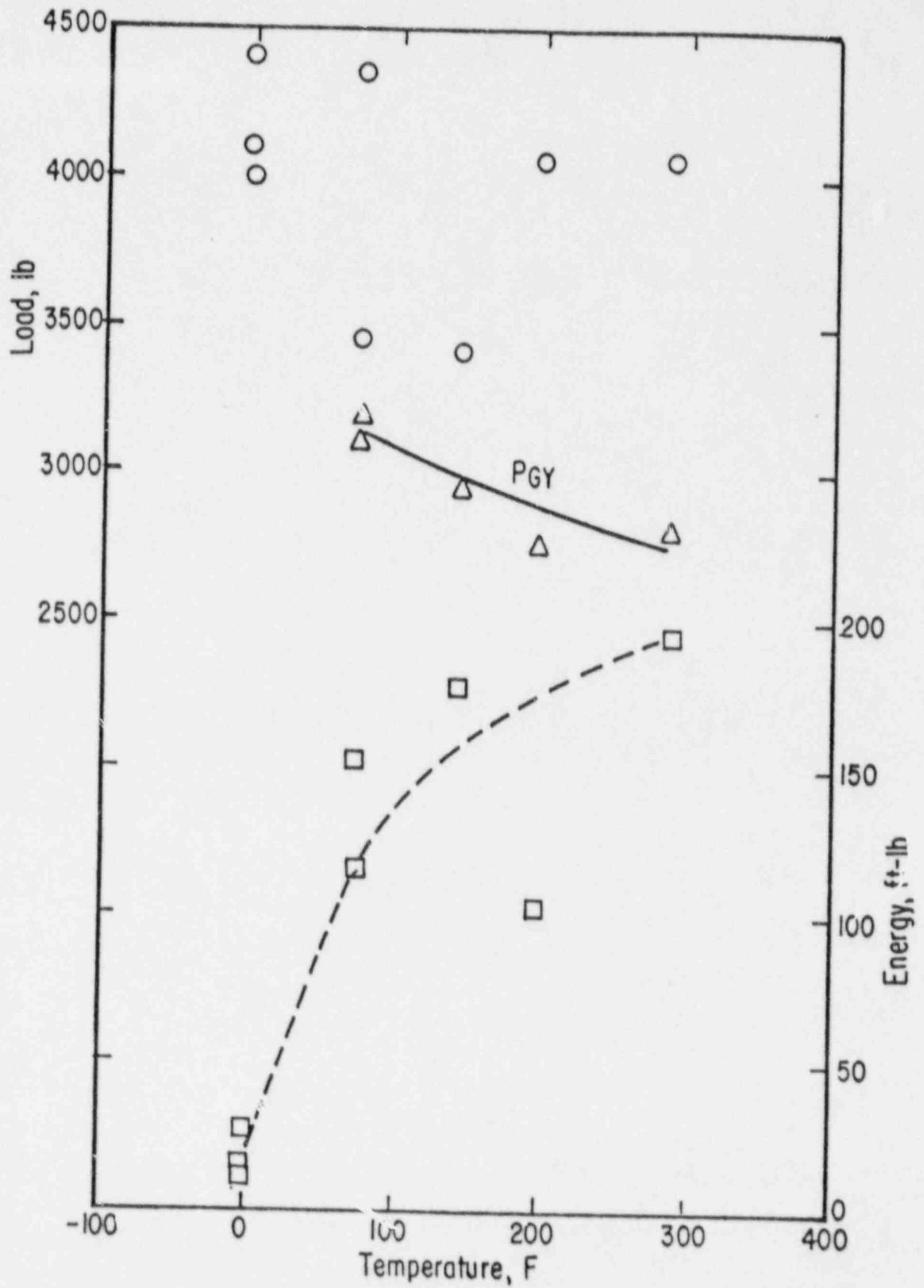


FIGURE E-8. INSTRUMENTED CHARPY LOAD-TEMPERATURE AND IMPACT ENERGY-TEMPERATURE CURVES FOR POINT BEACH UNIT NO. 2 HEAT AFFECTED ZONE METAL